

## Benzimidazole Derivatives as New Serotonin 5-HT<sub>6</sub> Receptor Antagonists. Molecular Mechanisms of Receptor Inactivation

Tania de la Fuente,<sup>†</sup> Mar Martín-Fontecha,<sup>†</sup> Jessica Sallander,<sup>‡</sup> Bellinda Benhamú,<sup>†</sup> Mercedes Campillo,<sup>‡</sup> Rocío A. Medina,<sup>†</sup> Lucie P. Pellissier,<sup>§</sup> Sylvie Claeysen,<sup>§</sup> Aline Dumuis,<sup>§</sup> Leonardo Pardo,<sup>\*,‡</sup> and María L. López-Rodríguez<sup>\*,†</sup>

<sup>†</sup>Departamento de Química Orgánica I, Facultad de Ciencias Químicas, Universidad Complutense de Madrid, E-28040 Madrid, Spain,

<sup>‡</sup>Laboratori de Medicina Computacional, Unitat de Bioestadística, Facultat de Medicina, Universitat Autònoma de Barcelona, E-08193

Bellaterra, Barcelona, Spain, and <sup>§</sup>Département de Neurobiologie, Institut de Génomique Fonctionnelle, CNRS, Université de Montpellier, INSERM U661, F-34094 Montpellier, France

Received November 12, 2009

On the basis of our previously described pharmacophore model for serotonin 5-HT<sub>6</sub> receptor (5-HT<sub>6</sub>R) antagonists, we have designed, synthesized, and pharmacologically characterized a series of benzimidazole derivatives **1–20** that represent a new family of potent antagonists at the human 5-HT<sub>6</sub>R. Site-directed mutagenesis and a  $\beta_2$ -adrenoceptor-based homology model of the 5-HT<sub>6</sub>R were used to predict the mode of binding of antagonist SB-258585 and the new synthesized ligands. Substitution of W6.48, F6.52, or N6.55 by Ala fully impedes compound **4** to block 5-HT-induced activation. Thus, we propose that D3.32 in TM 3 anchors the protonated piperazine ring, the benzimidazole ring expands parallel to EL 2 to hydrogen bond N6.55 in TM 6, and the aromatic ring is placed between TMs 3 and 5 in CH<sub>2</sub>-containing compounds and between TMs 3 and 6 in CO-containing compounds. This combined experimental and computational study has permitted to propose the molecular mechanisms by which the new benzimidazole derivatives act as 5-HT<sub>6</sub>R antagonists.

### Introduction

Serotonin (5-hydroxytryptamine, 5-HT) research is now more than 50 years old<sup>1–3</sup> but still represents one of the most attractive areas in medicinal chemistry.<sup>4</sup> Fourteen serotonin receptor subtypes have been identified so far that are classified into seven families (5-HT<sub>1–7</sub>)<sup>5,6</sup> based on amino acid sequences, pharmacology, and intracellular mechanisms. With the exception of the ionotropic 5-HT<sub>3</sub> receptor, all of the 5-HT subtypes are G protein-coupled receptors (GPCRs<sup>a</sup>).<sup>7–10</sup> To date many serotonergic agents acting at 5-HT<sub>1–4</sub> receptors are clinically used<sup>11</sup> for the treatment of certain central nervous system (CNS) illnesses. One of the most recent additions to the family of serotonin receptors is the human 5-HT<sub>6</sub> receptor (h5-HT<sub>6</sub>R), which was cloned in 1996<sup>12,13</sup> as a gene codifying a polypeptide chain of 440 amino acids<sup>13,14</sup> that is positively coupled to the adenylate cyclase<sup>15–17</sup> cascade via the G<sub>s</sub> protein. The high affinity of several antipsychotic and antidepressant agents<sup>13,18,19</sup> boosted the first studies exploring the 5-HT<sub>6</sub>R potential for the treatment of schizophrenia and bipolar affective disorder. However, contradictory results<sup>19</sup> were obtained about the role of the receptor in these therapeutic indications. Later on, 5-HT<sub>6</sub>R function was asso-

ciated with the control of cholinergic neurotransmission,<sup>20,21</sup> which prompted much interest into the possible implication of the receptor in cognitive impairment<sup>19,22,23</sup> (memory and learning) related to neurological diseases such as Alzheimer's. In the last five years, it has been shown that selective 5-HT<sub>6</sub>R ligands are able to reduce food intake,<sup>24,25</sup> although this effect had been unnoticed in early studies. Thus, the 5-HT<sub>6</sub>R has emerged as a promising target for the treatment of obesity and related metabolic syndrome,<sup>19,22,26</sup> a disease with an increasing global prevalence and high unmet clinical need. Clearly, there is much evidence that the h5-HT<sub>6</sub>R is involved in the pathogenesis of CNS diseases<sup>4,19,22,23,26,27</sup> related to cognitive or eating disorders, so it appears to be an attractive therapeutic target that should be exploited for drug development. Because it is known to be expressed almost exclusively in the CNS<sup>18,28–31</sup> and mainly in the olfactory tubercle, striatum, nucleus accumbens, and hippocampus, it is possible that new therapeutic agents targeting this receptor might have relatively few peripheral side effects. The first 5-HT<sub>6</sub>R antagonists Ro 04-6790,<sup>32</sup> Ro 63-0563,<sup>32</sup> and **46** (SB-258585)<sup>33</sup> (Chart 1), were identified in the late 1990s by high-throughput screening at Roche and GlaxoSmithKline. Soon afterward, Glennon et al.,<sup>34–37</sup> pioneering in the synthesis of 5-HT<sub>6</sub>R ligands, reported the first selective agonist EMDT<sup>35</sup> and antagonist MS-245<sup>36</sup> (Chart 1), concurrently discovered by Merck Sharp & Dohme.<sup>38</sup> Since then, the number of patent applications and scientific publications concerning the 5-HT<sub>6</sub>R experienced a dizzying growth, mostly in the past few years. At present, several research groups from both academia and the pharmaceutical industry have contributed to the development of structurally different 5-HT<sub>6</sub>R agonists

\*To whom correspondence should be addressed. For M.L.L.-R.: phone, 34-91-3944239; fax, 34-91-3944103; E-mail: mluzlr@quim.ucm.es. For L.P.: phone, 34-93-5812797; fax, 34-93-5812344; E-mail: Leonardo.Pardo@uab.es.

<sup>a</sup>Abbreviations: GPCR, G protein-coupled receptor; CNS, central nervous system; h5-HT<sub>6</sub>R, human 5-HT<sub>6</sub> receptor; PI, positive ionizable atom; HBA, H-bonding acceptor group; HYD, hydrophobic; TM, transmembrane helix; EL, extracellular loop; SEM, 2-(trimethylsilyl)ethoxymethyl; BOC, *tert*-butoxycarbonyl; WT, wild-type.

and antagonists<sup>4,19,22,26,27</sup> (such as WAY-181187, E-6801 and SB-357134, Chart 1), which have been used as pharmacological tools to study the receptor. To our knowledge,<sup>26</sup> eight of these compounds have entered clinical trials, and five of them are still under active development in phase I or II for the treatment of cognitive dysfunction associated with Alzheimer's disease or schizophrenia as well as for the treatment of obesity. However, no 5-HT<sub>6</sub>R ligand has been marketed so far and the search for new compounds acting at this receptor remains an area of high interest for medicinal chemists, aiming at either highly selective agents or compounds combining 5-HT<sub>6</sub>R activity with other serotonin activities thought to be beneficial for the treatment of CNS disorders.

In this context, we are involved in a project aimed at the development of new serotonin 5-HT<sub>6</sub>R ligands using a rational approach. As a starting point, using Catalyst software,<sup>39</sup> we generated a ligand-based pharmacophore model for 5-HT<sub>6</sub>R antagonism<sup>40</sup> from a training set of 45 structurally diverse compounds previously described. On the basis of

this model, here we have designed new benzimidazole derivatives containing a piperazine ring, either a carbonyl (–CO–) or a methylene (–CH<sub>2</sub>–) group, and an aromatic ring (benzene or naphthalene) (Figure 1). We report the synthesis of new compounds 1–20 and their binding affinity for the 5-HT<sub>6</sub>R (Table 1). The identified ligands have been characterized as antagonists in COS-7 cells transfected with the h5-HT<sub>6</sub>R, representing a new family of 5-HT<sub>6</sub>R antagonists. Site-directed mutagenesis and a  $\beta_2$ -adrenoceptor-based homology model of the 5-HT<sub>6</sub>R were used to predict the mode of binding of these ligands. This combined experimental and computational study has permitted us to propose the molecular mechanisms by which the new benzimidazole derivatives act as 5-HT<sub>6</sub>R antagonists.

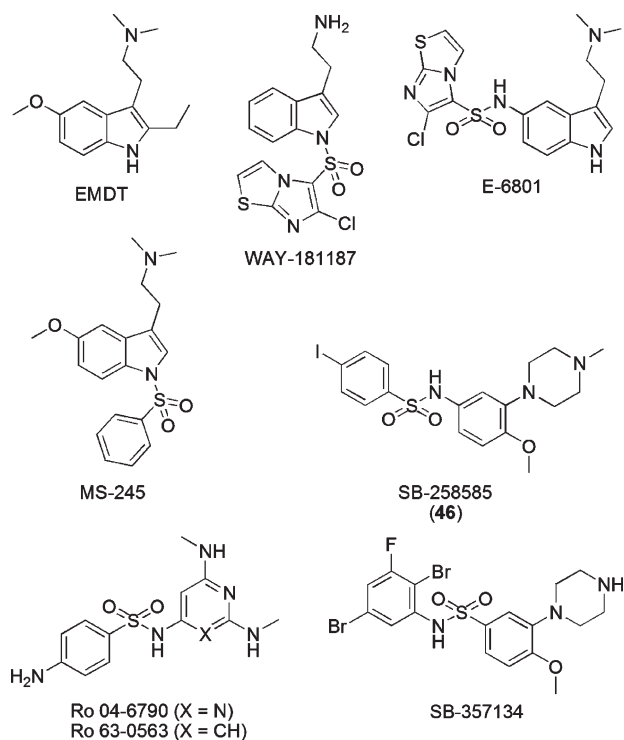
## Results and Discussion

### Pharmacophore-Based Design of New 5-HT<sub>6</sub>R Ligands.

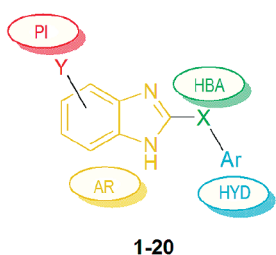
Our previously reported 3-D pharmacophore model for 5-HT<sub>6</sub>R antagonists showed four key pharmacophore elements: a positive ionizable atom (PI), an aromatic ring-hydrophobic site (AR), a hydrogen bond acceptor group (HBA), and a hydrophobic site (HYD).<sup>40</sup> On the basis of these structural requirements, we have designed a series of new compounds (Figure 1A) that contain a piperazine ring as PI, the AR feature is a benzimidazole system, the HBA feature is a carbonyl group (X = CO), and a benzene or naphthalene ring as HYD. Hence, the designed derivatives could represent a new structural class of 5-HT<sub>6</sub>R ligands, containing a benzimidazole scaffold in the central core. In the new compounds, the piperazine ring is attached to the benzimidazole system at either position 4 or position 5, providing two different orientations of the AR, HBA, and HYD moieties relative to the receptor-anchoring PI group. Figure 1B shows designed compound 3: Y = 4-(piperazin-1-yl), X = CO, Ar = 1-naphthyl mapped onto the 3-D model. Additionally, compounds lacking the HBA feature or the HYD region were studied in order to assess the influence of these pharmacophore elements on the binding to the receptor. Therefore, we also synthesized analogues (Figure 1A) where the carbonyl group (X = CO) was replaced by a methylene (X = CH<sub>2</sub>) with no hydrogen bond accepting capability or where the Ar moiety was missing (X = H).

**Synthesis.** The synthesis of new benzimidazole derivatives 1–20 (Figure 1A, Table 1) was performed by using two different strategies, depending on the nature of X moiety (X = CH<sub>2</sub> or X = CO, see Schemes 1–3). Compounds 10–20 (X = CH<sub>2</sub>) were obtained by nucleophilic

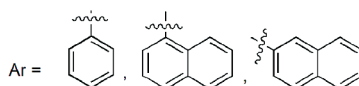
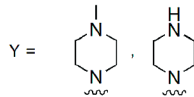
**Chart 1.** Structures of 5-HT<sub>6</sub>R Agonists and Antagonists



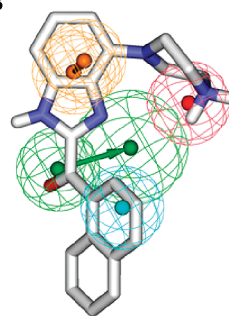
**A**



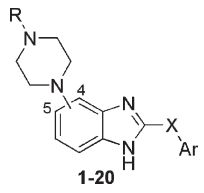
X = CO, CH<sub>2</sub>



**B**

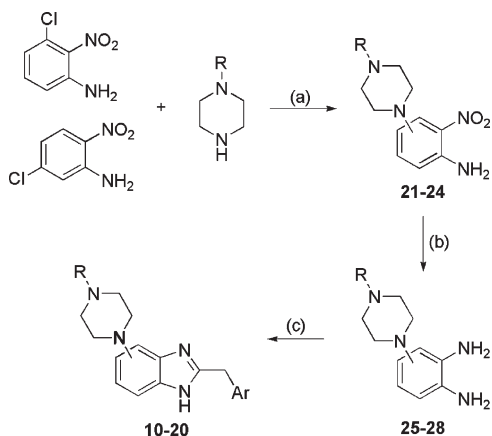


**Figure 1.** A previously reported 3-D pharmacophore model for 5-HT<sub>6</sub>R antagonists showed four key structural elements: a positive ionizable atom (PI, red), an aromatic ring-hydrophobic site (AR, yellow), a hydrogen bond acceptor group (HBA, green), and a hydrophobic site (HYD, blue). (A) Pharmacophore-based designed benzimidazole derivatives 1–20. (B) Designed compound 3: Y = 4-(piperazin-1-yl), X = CO, Ar = 1-naphthyl mapped onto the pharmacophore model.

**Table 1.** Binding Affinity of Synthesized Compounds 1–20 at the h5-HT<sub>6</sub>R


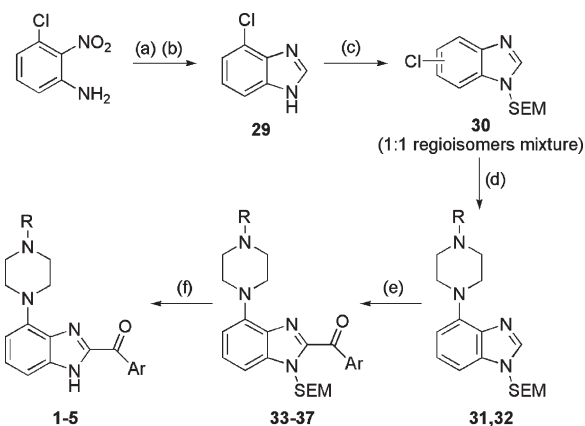
compd	position	R	X	Ar	$K_i \pm \text{SEM}$ (nM) <sup>a</sup>
1	4	H	CO	phenyl	> 1000
2	4	CH <sub>3</sub>	CO	phenyl	> 1000
3	4	H	CO	1-naphthyl	13 ± 1
4	4	CH <sub>3</sub>	CO	1-naphthyl	34 ± 2
5	4	CH <sub>3</sub>	CO	2-naphthyl	> 1000
6	5	CH <sub>3</sub>	CO	phenyl	> 1000
7	5	CH <sub>3</sub>	CO	1-naphthyl	> 1000
8	5	CH <sub>3</sub>	CO	2-naphthyl	> 1000
9	5	H	CO	2-naphthyl	> 1000
10	4	H	CH <sub>2</sub>	phenyl	58 ± 3
11	4	CH <sub>3</sub>	CH <sub>2</sub>	phenyl	66.8 ± 0.7
12	4	H	CH <sub>2</sub>	1-naphthyl	16 ± 2
13	4	CH <sub>3</sub>	CH <sub>2</sub>	1-naphthyl	36.22 ± 0.08
14	4	CH <sub>3</sub>	CH <sub>2</sub>	2-naphthyl	49 ± 3
15	5	H	CH <sub>2</sub>	phenyl	> 1000
16	5	CH <sub>3</sub>	CH <sub>2</sub>	phenyl	> 1000
17	5	H	CH <sub>2</sub>	1-naphthyl	> 1000
18	5	CH <sub>3</sub>	CH <sub>2</sub>	1-naphthyl	> 1000
19	5	H	CH <sub>2</sub>	2-naphthyl	> 1000
20	5	CH <sub>3</sub>	CH <sub>2</sub>	2-naphthyl	> 1000

<sup>a</sup> Values are the mean of two to four experiments performed in triplicate.

**Scheme 1<sup>a</sup>**

<sup>a</sup> Reagents and conditions: (a) Cs<sub>2</sub>CO<sub>3</sub> or K<sub>2</sub>CO<sub>3</sub>, DMF, 120 °C, 24 h, 40% to quantitative yield; (b) H<sub>2</sub>, Pd(C), MeOH, rt, 24 h, 89% to quantitative yield; (c) ArCH<sub>2</sub>CHO, Yb(OTf)<sub>3</sub>·2H<sub>2</sub>O, CH<sub>2</sub>Cl<sub>2</sub>, rt, overnight, 42–75%.

substitution of 3-chloro- or 5-chloro-2-nitroaniline with piperazine or 1-methylpiperazine, followed by catalytic hydrogenation of the resulting piperazinyl-2-nitroanilines **21–24** and subsequent oxidative cyclization of the obtained *o*-phenylenediamines **25–28** with the appropriate readily available arylaldehydes (Scheme 1). On the other hand, those benzimidazole derivatives having a carbonyl group (X = CO, **1–9**) were synthesized by butyllithium-mediated acylation at the 2-position of *N*-protected derivatives followed by removal of 2-(trimethylsilyl)ethoxymethyl (SEM) or *tert*-butoxycarbonyl (BOC) groups (Schemes 2 and 3).

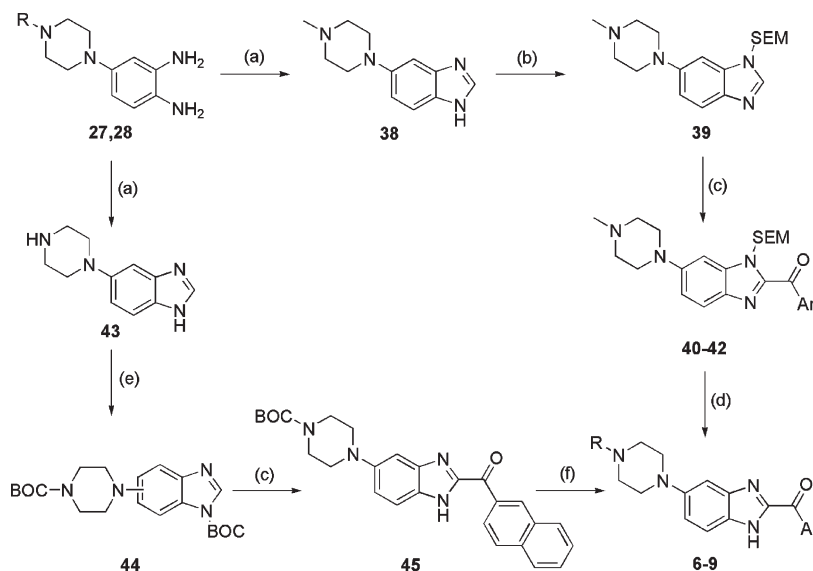
**Scheme 2<sup>a</sup>**

<sup>a</sup> Reagents and conditions: (a) SnCl<sub>2</sub>, HCl, rt, 3 h, quantitative yield; (b) HCOOH, H<sub>2</sub>O, 100 °C, 3 h, quantitative yield; (c) SEMCl, K<sub>2</sub>CO<sub>3</sub>, DMF, 0 °C to rt, 3 h, quantitative yield; (d) 1-BOC-piperazine or 1-methylpiperazine, NaO<sup>t</sup>Bu, Pd<sub>2</sub>dba<sub>3</sub>, P(<sup>t</sup>Bu)<sub>3</sub>, *o*-xylene, 110 °C, 24 h, 43–49%; (e) ArCOOR, BuLi, THF, –78 °C to rt, overnight, 21–59%; (f) BCl<sub>3</sub>, CH<sub>2</sub>Cl<sub>2</sub>, rt, 5 h, 50–64%.

Thus, the reduction of commercially available 3-chloro-2-nitroaniline, Phillips cyclization, and SEM protection of the obtained 4-chlorobenzimidazole (**29**)<sup>41,42</sup> afforded a nonseparable mixture of *N*-protected regioisomers **30**, in a 1:1 ratio (Scheme 2). Subsequent Pd(0)-catalyzed coupling<sup>43</sup> of **30** with 1-BOC- or 1-methylpiperazine yielded only 4-substituted intermediates **31,32**. Finally, derivatives **31,32** were acylated via butyllithium deprotonation, and SEM or BOC groups were subsequently removed to obtain desired compounds **1–5** (X = CO). Similarly, the cyclization of *o*-phenylenediamines **27,28**,<sup>44</sup> followed by the protection of 5-substituted benzimidazoles **38,43** and the 2-acylation of *N*-protected derivatives **39,44**, afforded final compounds **6–9** (X = CO) after deprotection of intermediates **40–42,45** (Scheme 3).

**Binding Affinities and Structure–Affinity Relationships.**

Target compounds **1–20** were assessed for in vitro affinity at the h5-HT<sub>6</sub>R by radioligand binding assays, using [<sup>3</sup>H]LSD in transfected HEK-293 cells (see Experimental Section for details). The competitive inhibition assays were first performed at a fixed dose of 10<sup>–6</sup> M, and the complete dose–response curve, at six different concentrations of the ligand, was determined for those compounds that presented a displacement of the radioligand over 50%. The inhibition constant  $K_i$  was calculated from the IC<sub>50</sub> value using the Cheng–Prusoff equation,<sup>45</sup> and the values in Table 1 are the mean of two–four experiments. Compounds binding the 5-HT<sub>6</sub>R were tested for selectivity over the 5-HT<sub>7</sub> receptor, using [<sup>3</sup>H]LSD in transfected HEK-293 cells (see Experimental Section for details), and found to be inactive ( $K_i > 500$  nM) at the 5-HT<sub>7</sub>R. The following structure–affinity relationships can be drawn from the 5-HT<sub>6</sub>R binding affinity data presented in Table 1. Most of the 4-substituted benzimidazole derivatives show high affinity ( $K_i = 13–66.8$  nM), whereas 5-substituted analogues are inactive ( $K_i > 1000$  nM). These experimental data show that 4-substituted benzimidazoles display a favorable orientation of the AR, HBA, and HYD moieties relative to the receptor-anchoring PI group. In 4-substituted derivatives containing a carbonyl group as HBA (**1–5**: X = CO), only compounds **3** and **4**, both containing 1-naphthyl ring as HYD moiety, show 5-HT<sub>6</sub>R affinity [ $K_i$ (**3**) = 13 nM;  $K_i$ (**4**) = 34 nM].

Scheme 3<sup>a</sup>

<sup>a</sup> Reagents and conditions: (a) HCOOH, H<sub>2</sub>O, 100 °C, 3 h, 60–87%; (b) (i) SEMCl, NaH, DMF, 0 °C to rt, 3 h, (ii) SiO<sub>2</sub> column chromatography (CH<sub>2</sub>Cl<sub>2</sub>/EtOH, 9:1), 44%; (c) ArCOOR, BuLi, THF, –78 °C to rt, overnight, 33–63%; (d) BCl<sub>3</sub>, CH<sub>2</sub>Cl<sub>2</sub>, rt, 5 h, 65–77%; (e) BOC<sub>2</sub>O, DMAP, Et<sub>3</sub>N, rt, overnight, 69%; (f) TFA, CH<sub>2</sub>Cl<sub>2</sub>, rt, 5 h, quantitative yield.

In contrast, phenyl [ $K_i(\mathbf{1}) > 1000$  nM vs  $K_i(\mathbf{3}) = 13$  nM,  $K_i(\mathbf{2}) > 1000$  nM vs  $K_i(\mathbf{4}) = 34$  nM] is insufficient for high-affinity binding, and the 2-naphthyl [ $K_i(\mathbf{5}) > 1000$  nM vs  $K_i(\mathbf{4}) = 34$  nM] aromatic system is not tolerated at the HYD region. However, when the carbonyl group is replaced by a methylene moiety all 4-substituted compounds (**10–14**; X = CH<sub>2</sub>) display affinity for the 5-HT<sub>6</sub>R ( $K_i = 16$ –66.8 nM). These results show that the hydrogen bonding capability proposed for HBA pharmacophore element is not essential for the binding of this new family of ligands to the 5-HT<sub>6</sub>R. Also, comparison of the affinity data obtained for compounds **4** (X = CO,  $K_i = 34$  nM) vs **13** (X = CH<sub>2</sub>,  $K_i = 36.22$  nM) and **3** (X = CO,  $K_i = 13$  nM) vs **12** (X = CH<sub>2</sub>,  $K_i = 16$  nM) suggest that the aromatic ring (Ar) is accommodated at different parts of the receptor for compounds with X = CO and X = CH<sub>2</sub> (see Computer-Based Analysis of the Structure–Affinity Relationships). The inactivity of 4-(4-methylpiperazin-1-yl)-1*H*-benzimidazole ( $K_i > 1000$  nM, data not shown), lacking the aromatic ring Ar, supports the hypothesis that the presence of HYD region is important for the receptor binding.

**Functional Activity of 5-HT<sub>6</sub>R Ligands.** Compounds displaying affinity for the 5-HT<sub>6</sub>R were evaluated for their functional profile by determining the adenylate cyclase activity in COS-7 cells expressing the human receptor. Cells were treated with the ligand for 10 min at 37 °C, in the absence (agonist effect) or the presence (antagonist effect) of serotonin (100 μM), and the cAMP content was then quantified by homogeneous time-resolved fluorescence (HTRF) (see Experimental Section for details). Adenylate cyclase activity is expressed as the percentage of the maximal effect obtained with serotonin alone. All assayed compounds show a dose-dependent effect in the presence of 5-HT and no effect in the absence of 5-HT, indicating their antagonist profile. The  $K_i$  values in Table 2 are the mean of three experiments, using eight different concentrations of the tested compound. These data ( $K_i = 5$ –31 nM) show that 4-substituted benzimidazoles represent a new family of potent 5-HT<sub>6</sub>R antagonists.

**Defining the Mode of Binding of Ligand 4 by Site-Directed Mutagenesis and Computational Modeling.** Figure 2 shows

**Table 2.** Potency of New 5-HT<sub>6</sub>R Antagonists

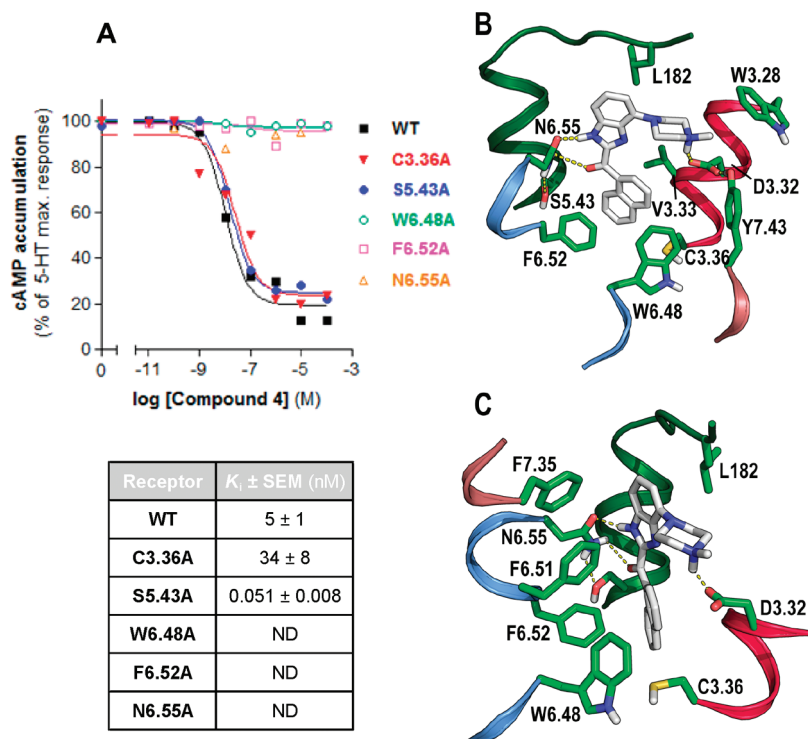
compd	R	X	Ar	$K_i \pm$ SEM (nM) <sup>a</sup>
<b>3</b>	H	CO	1-naphthyl	15 ± 2
<b>4</b>	CH <sub>3</sub>	CO	1-naphthyl	5 ± 2
<b>10</b>	H	CH <sub>2</sub>	phenyl	31 ± 4
<b>11</b>	CH <sub>3</sub>	CH <sub>2</sub>	phenyl	16 ± 5
<b>12</b>	H	CH <sub>2</sub>	1-naphthyl	16 ± 3
<b>13</b>	CH <sub>3</sub>	CH <sub>2</sub>	1-naphthyl	27 ± 3
<b>14</b>	CH <sub>3</sub>	CH <sub>2</sub>	2-naphthyl	17 ± 4

<sup>a</sup> Values are the mean of three experiments performed in triplicate.

the sequence alignment of transmembrane helices (TMs) 3, 5, 6, and 7 and extracellular loop (EL) 2 for β<sub>1</sub>- and β<sub>2</sub>-adrenergic receptors, selected serotonin receptors, and the 5-HT<sub>6</sub>R. These domains form the ligand binding site in the crystal structures of β<sub>1</sub>-<sup>46</sup> and β<sub>2</sub>-<sup>47,48</sup> adrenergic receptors, as they were previously identified by site-directed mutagenesis.<sup>49</sup> To characterize the amino acid residues of the 5-HT<sub>6</sub>R involved in the binding of ligand **4**, mutagenesis assays were performed with Ala substitution at C3.36, S5.43, W6.48, F6.52, and N6.55 sites. Receptor expression levels at the plasma membrane relative to the expression of wild-type (WT) receptor were determined by an ELISA assay. These mutant receptors are expressed at the 80–110% range with the exception of W6.48A (30%). Figure 3A shows the antagonist activity of **4** relative to 5-HT-induced activation in the five mutant receptors and in the WT 5-HT<sub>6</sub>R. Notably, the substitution of W6.48, F6.52, or N6.55 by Ala fully impedes compound **4** to block 5-HT-induced activation. The C3.36A mutation decreases the antagonist activity of the ligand by 7-fold [ $K_i(\text{WT}) = 5$  nM vs  $K_i(\text{C3.36A}) = 34$  nM].

	TM3 3.28 - 3.37	EL2	TM5 5.42 - 5.50	TM6 6.47 - 6.55	TM7 7.35 - 7.40
$\beta_1$	WTSIDVLCVT	CDFVTNR	SSIISFYIP	CWLEPFLVN	FVAFNW
$\beta_2$	WTSIDVLCVT	CDFFTNQ	SSIISFYVP	CWLEPFIYN	YILLNW
5-HT <sub>1A</sub>	FIALDVLCCT	CTISKDH	STFGAFYIP	CWLEPFIYA	GAIINW
5-HT <sub>2A</sub>	WIYLDVLFST	CLLA-DD	GSFVSFFIP	MWCPEFITN	LNVEVW
5-HT <sub>4</sub>	RTSIDVLLIT	CVFMVNK	CSVVAFYIP	CWAEFFVTN	WTAEVW
5-HT <sub>7</sub>	FIAMDVMCCT	CLISQDF	STAVAFYIP	CWLEPFLLS	ERTFLW
5-HT <sub>6</sub>	WTAFDVMCCS	CRLLASL	ASGLTFFLP	TWLEPFFVAN	FDVLTW

**Figure 2.** Sequence alignment of TMs 3, 5–7 and EL 2 of  $\beta_1$ - and  $\beta_2$ -adrenergic receptors, and serotonin 5-HT<sub>1A</sub>, 5-HT<sub>2A</sub>, 5-HT<sub>4</sub>, 5-HT<sub>7</sub>, and 5-HT<sub>6</sub> receptors. Residues referenced in the manuscript are boxed. The highly conserved WxPFF motif in TM 6 is shown in dark gray.

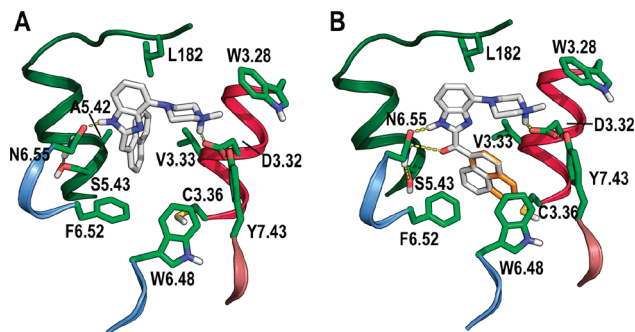


**Figure 3.** (A) The antagonist activity of compound **4** was tested relative to 5-HT-induced activation in WT 5-HT<sub>6</sub>R and C3.36A, S5.43A, W6.48A, F6.52A, and N6.55A mutant receptors. The antagonist effect is represented as the percentage of inhibition of 5-HT (100  $\mu$ M)-induced stimulation of cAMP taken as 100%. Each value represents the mean  $\pm$  SEM determined from three independent experiments performed in triplicate. The inhibition constant  $K_i$  was calculated from the  $IC_{50}$  value using the Cheng–Prusoff equation.  $IC_{50}$  was assessed as the concentration required to inhibit 50% of 5-HT (100  $\mu$ M)-induced stimulation of cAMP.  $EC_{50}$  values of 5-HT on WT, C3.36A, and S5.43A receptors were  $5 \pm 1$  nM,  $0.8 \pm 0.1$   $\mu$ M, and  $3 \pm 1$  nM, respectively. (B,C) Computational model of the complex between ligand **4** (in white) and the 5-HT<sub>6</sub>R. In this model, D3.32 anchors the protonated piperazine ring, the benzimidazole ring hydrogen bonds N6.55 and interacts with F6.51, F7.35, and L182 in EL 2, and the aromatic naphthalene ring enters into a small cavity between TMs 3 and 6 to interact with V3.33, W6.48, and F6.52. Panels B and C are rotated 90°. The color code of the helices is: TM 3 (red), 5 (green), 6 (blue), and 7 (brown).

Surprisingly, the S5.43A mutation substantially increases the antagonist activity of **4** by 98-fold [ $K_i(\text{WT}) = 5$  nM vs  $K_i(\text{S5.43A}) = 0.051$  nM].

To understand these observed effects at the molecular level, we constructed a computer 3-D model of the complex between compound **4** and a  $\beta_2$ -adrenoceptor-based model of the 5-HT<sub>6</sub>R (see Experimental Section). In this model (Figure 3B), D3.32 anchors the protonated piperazine ring, the benzimidazole ring expands toward TM 6, parallel to EL 2, to hydrogen bond O<sub>8</sub> of the key N6.55, the coplanar carbonyl group also hydrogen bonds the N<sub>8</sub>-H moiety of N6.55, and the aromatic naphthalene ring enters deeply into a small cavity between TMs 3 and 6 to form edge-to-face interactions with the key W6.48 and F6.52 side chains in

TM 6. This computational model explains the experimentally determined importance of W6.48, F6.52, and N6.55 of the 5-HT<sub>6</sub>R in the binding of ligand **4** (Figure 3A). The finding that the S5.43A mutation enhances the activity of **4** (Figure 3A) is attributed to the fact that S5.43 hydrogen bonds N6.55 (Figure 3B); thus, the mutation at this site increases the flexibility of N6.55, favoring its interaction with **4**. Other significant interactions between compound **4** and the 5-HT<sub>6</sub>R, as revealed by the computational model, are: the interaction between the highly polar methyl group attached to the protonated piperazine ring and W3.28, the interaction of the aromatic naphthalene ring with V3.33 in TM 3, and the interaction between the aromatic benzimidazole ring and F6.51 in TM 6, F7.35 in TM 7, and L182 in EL 2 (Figure 3B,C).



**Figure 4.** Computational models of the complexes between ligand **13** (A) and **4** (B) and the 5-HT<sub>6</sub>R. An important feature of these molecules is the linker between the benzimidazole ring and the terminal aromatic ring. The methylene unit (–CH<sub>2</sub>–) of ligand **13** allows both rings to form an angle of approximately 90° (A), whereas the carbonyl group (–CO–) of ligand **4** enforces both aromatic domains to be coplanar (B). In CH<sub>2</sub>-containing compounds, the aromatic ring is located between TMs 3 and 5, to interact with V3.33 and A5.42 (A). In CO-containing compounds, the aromatic moiety is located between TMs 3 and 6, interacting with V3.33, W6.48, and F6.52 (B). 2-Naphthyl (in orange) is not tolerated within the cavity between TMs 3 and 6 due to the clash with TM 3 (B). The color code of the helices is: TM 3 (red), 5 (green), 6 (blue), and 7 (brown).

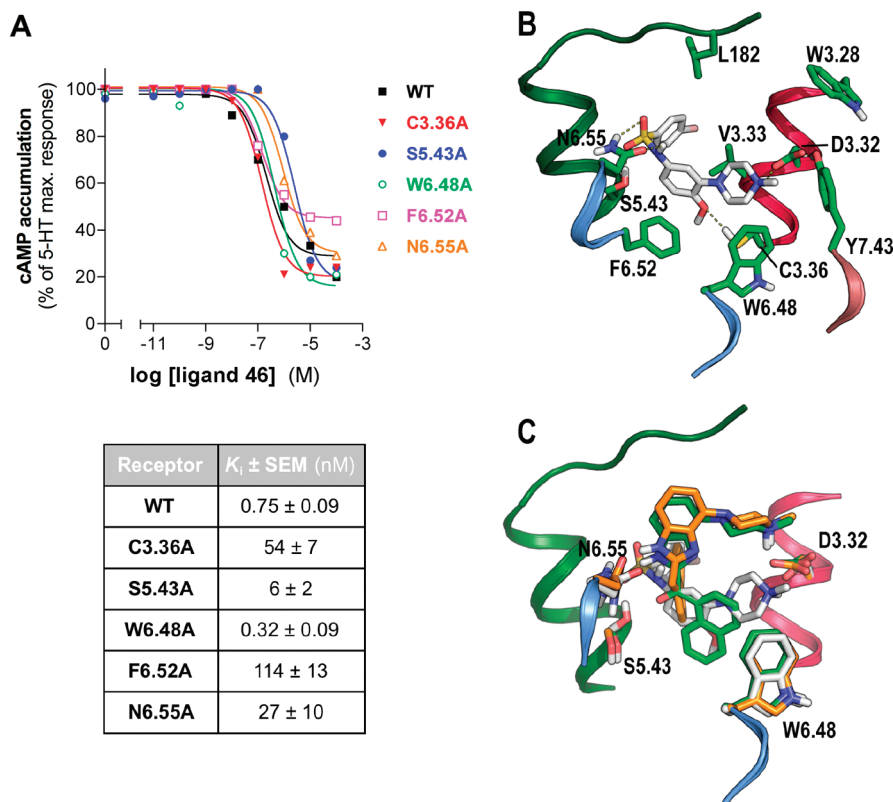
**Computer-Based Analysis of the Structure–Affinity Relationships.** In an attempt to get a better understanding of the above-described structure–affinity relationships, we have performed additional computational simulations of the complexes between 4-substituted benzimidazole derivatives and the 5-HT<sub>6</sub>R. Regarding HBA, replacement of the sp<sup>2</sup> carbonyl group (X = CO) by the sp<sup>3</sup> methylene unit (X = CH<sub>2</sub>) allows the benzimidazole ring and the aromatic systems (Ar = phenyl, 1-naphthyl, 2-naphthyl) in the HYD region to form an angle of approximately 90°. Thus, in compounds with X = CH<sub>2</sub>, the HYD moiety is located between TMs 3 and 5 to interact with the hydrophobic side chains of V3.33 and A5.42 (Figure 4A). In contrast, the Ar aromatic moiety in compounds containing X = CO is located between TMs 3 and 6, interacting with V3.33, W6.48, and F6.52 side chains (Figure 4B). The different location of the HYD feature in the receptor explains the observed different structure–affinity relationships at this pharmacophore element in both types of compounds (X = CH<sub>2</sub> or X = CO). Clearly, all tested aromatic rings phenyl, 1-naphthyl, and 2-naphthyl are permitted in the cavity between TMs 3 and 5 (X = CH<sub>2</sub>, Figure 4A), whereas phenyl and 1-naphthyl are permitted in the cavity between TMs 3 and 6 (X = CO, Figure 4B). In the cavity between TMs 3 and 6, the smaller phenyl ring, relative to 1-naphthyl, does not optimally interact with F6.52 (Figure 4B), resulting in the corresponding loss of affinity [*K<sub>i</sub>*(**1**) > 1000 nM, *K<sub>i</sub>*(**2**) > 1000 nM]. The presence of the 2-naphthyl system is not permitted because it clashes with TM 3 (see orange ring in Figure 4B), leading to an inactive analogue [*K<sub>i</sub>*(**5**) > 1000 nM].

**Comparison of the Binding of Ligand **46** with the Binding of Benzimidazole Derivatives **4** and **13** to the 5-HT<sub>6</sub>R.** Sulfonamide **46**<sup>33</sup> (Chart 1) is a commercially available potent 5-HT<sub>6</sub>R antagonist that contains the common piperazine ring as the PI pharmacophore element, a methoxyphenyl system as AR, a sulfonamide group as HBA, and a iodophenyl ring as HYD.<sup>40</sup> To compare the binding mode of this 5-HT<sub>6</sub>R antagonist with the binding mode of benzimidazole derivatives, we evaluated the antagonist activity of **46** in the C3.36A,

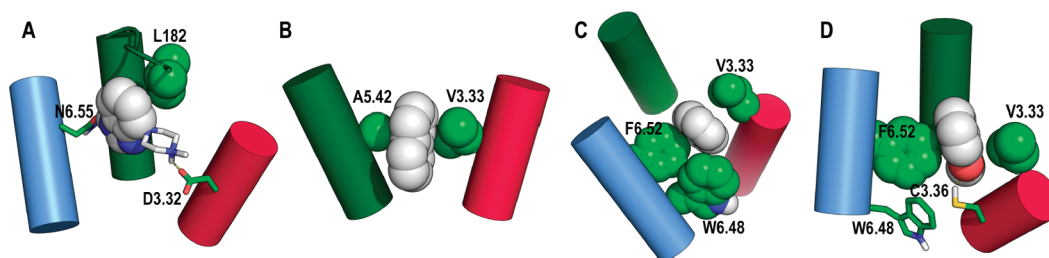
S5.43A, W6.48A, F6.52A, and N6.55A mutant receptors (Figure 5A). Clearly, with the only exception of W6.48A, all these mutations decrease the antagonist activity of **46**: 72-fold, relative to WT, in the C3.36A mutant receptor; 8-fold in S5.43A, 152-fold in F6.52A, and 36-fold in N6.55A (Figure 5A). These mutational data are compatible with a mode of binding of **46** to the 5-HT<sub>6</sub>R as depicted in Figure 5B: D3.32 anchors the protonated piperazine ring, the methoxyphenyl system interacts with F6.52, the methoxy group hydrogen bonds C3.36, the sulfonamide group hydrogen bonds both S5.43 and N6.55, and the substituted benzene interacts with the hydrophobic side chains of V3.33 and A5.42. Previously reported rhodopsin-based models have suggested that arylsulfonyltryptamines bind between TMs 1, 6, and 7,<sup>50</sup> the sulfonyl oxygens of MS-245 (Chart 1) bind S3.37 and T5.46,<sup>51</sup> or N6.55 in SB-357134 (Chart 1) and related sulfonamide derivatives.<sup>31,40</sup>

Figure 5C shows ligand **46** (white) and benzimidazole derivatives **4** (green) and **13** (orange) bound to the 5-HT<sub>6</sub>R for comparison purposes. With respect to the HBA feature, the large sulfonamide moiety of **46** is capable to hydrogen bond both S5.43 and N6.55 while the carbonyl group of compound **4** hydrogen bonds exclusively N6.55, which also binds the N–H of the benzimidazole ring (AR feature) of compounds **4** and **13**. Clearly, the piperazine-benzimidazole rings of **4** and **13** are placed near the extracellular side, parallel to EL 2, while the piperazine-methoxyphenyl rings of **46** are located deeper in the TM bundle. Notably, the methoxyphenyl system of **46** (AR feature) is placed at a similar position to that of the naphthalene ring (HYD feature) of compound **4**. On the other hand, the position of the HYD feature of **46** (iodophenyl ring) is similar to the HYD feature of compound **13** (naphthalene ring). Thus, the different location of the AR features in the binding site suggests that compounds **4** and **13** elicit their antagonist function by a different mechanism than ligand **46** (see below).

**Molecular Mechanisms of Receptor Inactivation.** The understanding of the molecular mechanisms by which these benzimidazole derivatives act as 5-HT<sub>6</sub>R antagonists, and GPCR function in general, is a key subject in medicinal chemistry. The recent knowledge of the molecular steps of agonist-induced GPCR activation (see Smit et al.<sup>52</sup> and Nygaard et al.<sup>53</sup> for recent reviews) facilitates this task. It has been proposed, from engineered GPCRs with metal ion binding sites, that TM 6 performs an inward movement of the extracellular part toward TM 3.<sup>54</sup> Thus, in the new family of 5-HT<sub>6</sub>R antagonists the role of the benzimidazole ring may be to maintain, by forming a hydrogen bond interaction with N6.55, TM 6 away from the center of the bundle (Figure 6A). In addition, L182 in EL 2 forms favorable C–H···π interactions<sup>55</sup> with the benzimidazole ring, which may serve to immobilize both EL 2 and TM 6 in the inactive conformation (Figure 6A). Similar interactions are observed between the antagonist cyanopindolol and the partial inverse agonist carazolol with the homologous F201<sup>46</sup> and F193<sup>48</sup> of the β<sub>1</sub>- and β<sub>2</sub>-adrenergic receptors, respectively. Fluorescence spectroscopy in the β<sub>2</sub>-adrenergic receptor provides evidence that agonist binding induces or stabilizes relocation of the extracellular side of TM 5 to facilitate binding of the catechol hydroxyls of the adrenergic agonists.<sup>56</sup> The Ar system in CH<sub>2</sub>-containing compounds is located between TMs 3 and 5, interacting with V3.33 and A5.42, and probably blocking these helices in the inactive conformation (Figure 6B).



**Figure 5.** (A) The antagonist activity of ligand **46** was tested relative to 5-HT-induced activation in WT 5-HT<sub>6</sub>R and C3.36A, S5.43A, W6.48A, F6.52A, and N6.55A mutant receptors. The antagonist effect is represented as the percentage of inhibition of 5-HT (100  $\mu$ M)-induced stimulation of cAMP taken as 100%. Each value represents the mean  $\pm$  SEM determined from three independent experiments performed in triplicate. The inhibition constant  $K_i$  was calculated from the  $IC_{50}$  value using the Cheng–Prusoff equation.  $IC_{50}$  was assessed as the concentration required to inhibit 50% of 5-HT (100  $\mu$ M)-induced stimulation of cAMP.  $EC_{50}$  values of 5-HT were  $5 \pm 1$  nM on WT,  $0.8 \pm 0.1$   $\mu$ M on C3.36A,  $3 \pm 1$  nM on S5.43A,  $1.1 \pm 0.1$  nM on W6.48A,  $0.18 \pm 0.06$   $\mu$ M on F6.52A, and  $45 \pm 2$  nM on N6.55A receptor. (B) Computational model of the complex between ligand **46** (in white) and the 5-HT<sub>6</sub>R. In this model, D3.32 anchors the protonated piperazine ring, the methoxyphenyl system interacts with F6.52, the methoxy group hydrogen bonds C3.36, the sulfonamide moiety hydrogen bonds both S5.43 and N6.55, and the iodophenyl ring interacts with the hydrophobic side chains of V3.33 and A5.42. (C) Comparison of the binding modes of ligand **46** (white) and benzimidazole derivatives **4** (green) and **13** (orange) to the 5-HT<sub>6</sub>R. The color code of the helices is: TM 3 (red), 5 (green), 6 (blue), and 7 (brown).



**Figure 6.** Molecular mechanisms of receptor inactivation. (A) The benzimidazole ring (in white spheres) impedes the proposed inward movement of the extracellular part of TM 6 toward TM 3 required for receptor activation.<sup>54</sup> The interaction of L182 in EL 2 with the benzimidazole ring may serve to immobilize both EL 2 and TM 6 in the inactive conformation. (B) The aromatic naphthalene ring (in white spheres) in CH<sub>2</sub>-containing compounds is located between TMs 3 and 5, interacting with V3.33 and A5.42, and probably blocking the movement of these helices necessary for receptor activation.<sup>56</sup> (C) The aromatic naphthalene ring (in white spheres) in CO-containing compounds is located between TMs 3 and 6, interacting with V3.33, W6.48, and F6.52. This mode of binding blocks the proposed rotamer toggle switch of W6.48 and the subsequent steps in the activation process.<sup>50</sup> (D) The methoxyphenyl system of ligand **46** (in white spheres) is located between TMs 3 and 6, interacting with V3.33, C3.36, and F6.52. The hydrogen bond between the methoxy group and C3.36 blocks the conformational transition of C3.36 toward TM 7 during the process of receptor activation.<sup>60</sup> The color code of the helices is: TM 3 (red), 5 (green), and 6 (blue).

In addition to these activation pathways, agonist binding might also trigger the rotamer toggle switch of W6.48 from pointing toward TM 7 to pointing toward the binding site crevice,<sup>49,57,58</sup> through the formation of specific hydrogen bonds.<sup>59</sup> The 1-naphthyl ring in CO-containing compounds occupies a small cavity between TMs 3 and 6 (Figure 6C) and

might act by blocking the proposed conformational transition of W6.48 and the subsequent steps in the activation process.<sup>52</sup> We have also shown that the conformational transition of W6.48 is accompanied, in a concerted manner, by the conformational transition of the side chain at position 3.36 from pointing toward TM 6 to pointing toward TM 7.<sup>60</sup>

Thus, the methoxy group of **46** might block receptor activation by hydrogen bonding C3.36 in the inactive conformation (Figure 6D). Accordingly, the C3.36A mutation has a significant effect in the antagonist activity of **46** (the effect for compound **4** is less significant), while the W6.48A mutation impairs the antagonist activity of compound **4** (the effect for ligand **46** is minor).

## Conclusions

On the basis of our previously described pharmacophore model for 5-HT<sub>6</sub>R antagonists,<sup>40</sup> we have identified benzimidazole derivatives as a new structural class of serotonin 5-HT<sub>6</sub>R ligands. Computational modeling and site-directed mutagenesis have allowed us to characterize the amino acid residues of 5-HT<sub>6</sub>R involved in ligand binding (Figure 3). The distinctive positively charged piperazine ring anchors the ligand to D3.32 in TM 3, whereas the benzimidazole ring is situated parallel to EL 2, to hydrogen bond N6.55 in TM 6 (Figures 3 and 4). An important feature of these molecules is the linker between the benzimidazole ring and the terminal Ar system (phenyl, 1-naphthyl, 2-naphthyl). The sp<sup>2</sup> carbonyl group (–CO–) enforces both aromatic domains to be coplanar, whereas the sp<sup>3</sup> methylene unit (–CH<sub>2</sub>–) allows the rings to form an angle of approximately 90°. Thus, in CH<sub>2</sub>-containing compounds, the Ar system is located between TMs 3 and 5, to interact with V3.33 and A5.42 (Figure 4A), whereas in CO-containing compounds, the Ar aromatic moiety is located between TMs 3 and 6, interacting with V3.33, W6.48, and F6.52 (Figure 4B). Both types of compounds display high binding affinity for the 5-HT<sub>6</sub>R as shown for ligands **12** [*K<sub>i</sub>*(**12**) = 16 nM] and **13** [*K<sub>i</sub>*(**13**) = 36 nM], having CH<sub>2</sub> as a linker, and ligands **3** [*K<sub>i</sub>*(**3**) = 13 nM] and **4** [*K<sub>i</sub>*(**4**) = 34 nM] containing CO (Table 1). The new compounds were pharmacologically characterized as potent 5-HT<sub>6</sub>R antagonists (*K<sub>i</sub>* = 5–31 nM).

This combined experimental and computational study has permitted to understand how ligand binding blocks receptor activation (Figure 6), which may contribute to the rational design of new compounds acting at the serotonin 5-HT<sub>6</sub>R. As some of the residues involved in ligand binding and receptor inactivation are strongly conserved, these findings can likely be extended to other members of the rhodopsin-like family of GPCRs.

## Experimental Section

**Chemistry.** Melting points (uncorrected) were determined on a Stuart Scientific electrothermal apparatus. Infrared (IR) spectra were measured on a Shimadzu-8300 or Bruker Tensor 27 instrument equipped with a Specac ATR accessory of 5200–650 cm<sup>-1</sup> transmission range; frequencies ( $\nu$ ) are expressed in cm<sup>-1</sup>. Nuclear magnetic resonance (NMR) spectra were recorded on a Bruker Avance 500 (<sup>1</sup>H, 500 MHz; <sup>13</sup>C, 125 MHz), Bruker Avance 300 AM. (<sup>1</sup>H, 300 MHz; <sup>13</sup>C, 75 MHz) or Bruker 200-AC spectrometer (<sup>1</sup>H, 200 MHz; <sup>13</sup>C, 50 MHz) at the UCM's NMR facilities. Chemical shifts ( $\delta$ ) are expressed in parts per million relative to internal tetramethylsilane; coupling constants (*J*) are in hertz (Hz). The following abbreviations are used to describe peak patterns when appropriate: s (singlet), d (doublet), t (triplet), m (multiplet), br (broad), app (apparent). Mass spectrometry (MS) was carried out on a Bruker LC-Esquire in electrospray mode (ESI) or a HP 5989 A in electron impact mode (EI, 70 eV). Elemental analyses (C, H, N) were obtained on a LECO CHNS-932 apparatus at the UCM's analysis services and were within 0.5% of the theoretical values, confirming a purity of at least 95% for all tested compounds. Analytical thin-layer chromatography (TLC) was

run on Merck silica gel plates (Kieselgel 60 F-254) with detection by UV light (254 nm), ninhydrin solution, or 10% phosphomolybdic acid solution in ethanol. Flash chromatography was performed on glass column using silica gel type 60 (Merck, particle 230–400 mesh) or on a Supelco VersaFlash station using silica gel cartridges (Supelco, particle size 20–45  $\mu$ m). Unless stated otherwise, starting materials, reagents, and solvents were purchased as high-grade commercial products from Sigma-Aldrich, Lancaster, Scharlab, or Panreac and were used without further purification. THF was distilled from sodium benzophenone ketyl and used immediately. Dichloromethane was distilled from calcium hydride.

The following compounds were synthesized according to described procedures: **23**,<sup>61</sup> **24**,<sup>44</sup> **28**,<sup>62</sup> and **29**,<sup>42</sup> and their spectroscopic data are in agreement with those previously described.

Spectroscopic data of all described compounds were consistent with the proposed structures. For series **1–8**, **10–20**, we include the data of compounds **5**, **6**, **8**, **11**, **12**, **15**, and **19**. For intermediates **25–28**, **33–37**, **40–42**, the data of compounds **26**, **35**, and **42** are described.

**General Procedure for the Synthesis of 2-Nitro- $\omega$ -piperazin-1-ylanilines (**21–24**).** To a solution of 3- or 5-chloro-2-nitroaniline (5.12 g, 29.5 mmol) in anhydrous DMF (70 mL), piperazine, or 1-methylpiperazine (78 mmol), Cs<sub>2</sub>CO<sub>3</sub>, or K<sub>2</sub>CO<sub>3</sub> (78 mmol) were added, respectively. The reaction was heated at 120 °C for 24 h. Upon cooling, the mixture was poured into ice-cold water and the solid was filtered, washed with cold water, and dried under vacuum. The solid was purified by column chromatography using the appropriate eluent, to afford pure **21–24**.

**2-Nitro-3-piperazin-1-ylaniline (21).** Obtained from 3-chloro-2-nitroaniline and piperazine, in 40% yield. Chromatography: CH<sub>2</sub>Cl<sub>2</sub>/EtOH, 8:2; mp 212–213 °C. IR (KBr) 3308, 1514, 1443. <sup>1</sup>H NMR (CDCl<sub>3</sub>,  $\delta$ ): 1.90 (br s, 1H), 3.01 (m, 8H), 4.95 (br s, 2H), 6.57 (d, *J* = 8.1, 2H), 7.14 (t, *J* = 8.1, 1H). <sup>13</sup>C NMR (CDCl<sub>3</sub>,  $\delta$ ) 46.2, 53.0, 109.3, 111.2, 122.0, 132.9, 142.9, 148.0. MS (ESI) 223.0 (M + H).

**3-(4-Methylpiperazin-1-yl)-2-nitroaniline (22).** Obtained from 3-chloro-2-nitroaniline and 1-methylpiperazine, in quantitative yield. Chromatography: CH<sub>2</sub>Cl<sub>2</sub>/EtOH, 9:1. IR (CHCl<sub>3</sub>) 3383, 1605, 1573, 1511, 1459. <sup>1</sup>H NMR (CDCl<sub>3</sub>)  $\delta$  2.32 (s, 3H), 2.53 (br t, *J* = 4.7, 4H), 3.01 (br t, *J* = 4.7, 4H), 4.80 (br s, 2H), 6.38 (d, *J* = 8.1, 2H), 7.11 (t, *J* = 8.1, 1H). <sup>13</sup>C NMR (CDCl<sub>3</sub>)  $\delta$  46.1, 51.7, 55.1, 109.1, 111.2, 121.3, 132.9, 142.6, 147.6. MS (ESI) 258.9 (M + Na).

**2-Nitro-5-piperazin-1-ylaniline (23).** Obtained from 5-chloro-2-nitroaniline and piperazine, in quantitative yield. Chromatography: CH<sub>2</sub>Cl<sub>2</sub>/EtOH, 9:1; mp 164–165 °C (lit.<sup>61</sup> 170 °C).

**5-(4-Methylpiperazin-1-yl)-2-nitroaniline (24).** Obtained from 5-chloro-2-nitroaniline and 1-methylpiperazine, in 89% yield. Chromatography: CH<sub>2</sub>Cl<sub>2</sub>/EtOH, 98:2; mp 153–154 °C (lit.<sup>44</sup> 156–157 °C).

**General Procedure for the Synthesis of  $\omega$ -Piperazin-1-ylbenzene-1,2-diamines (**25–28**).** To a suspension of **21–24** (1.3 mmol) in absolute MeOH (10 mL), 10% Pd(C) (25 mg) was added, and the reaction was hydrogenated at room temperature for 24 h, with an initial hydrogen pressure of 50 psi. The mixture was filtered over celite, and the solvent was evaporated to dryness to give **25–28**, which were used in the next step without further purification.

**3-Piperazin-1-ylbenzene-1,2-diamine (25).** Obtained from **21** in quantitative yield.

**3-(4-Methylpiperazin-1-yl)benzene-1,2-diamine (26).** Obtained from **22** in quantitative yield. IR (CHCl<sub>3</sub>) 3325, 1600, 1478, 1455. <sup>1</sup>H NMR (CDCl<sub>3</sub>)  $\delta$  2.31 (s, 3H), 2.60 (m, 4H), 2.94 (br t, *J* = 4.7, 4H), 6.54 (dd, *J* = 6.9, 1.4, 1H), 6.63–6.72 (m, 2H). <sup>13</sup>C NMR (CDCl<sub>3</sub>)  $\delta$  46.1, 51.3, 55.9, 111.6, 112.7, 118.9, 130.1, 134.4, 140.2. MS (ESI) 207.0 (M + H), 228.9 (M + Na).

**4-Piperazin-1-ylbenzene-1,2-diamine (27).** Obtained from **23** in quantitative yield.



**4-(4-Methylpiperazin-1-yl)benzene-1,2-diamine (28).** Obtained from **24** in 89% yield; mp 101–103 °C (lit.<sup>62</sup> 101–102 °C).

**General Procedure for the Synthesis of Compounds 29, 38, 43.** To a suspension of 3-chlorobenzene-1,2-diamine,<sup>41</sup> **27** or **28** (9.8 mmol) in water (14 mL), formic acid (1.2 mL, 29 mmol) was added and the mixture was heated at 100 °C for 3 h. After the complete disappearance of the starting material (tlc), the reaction was poured on ice and 1 M KOH was added until pH 9–10. The resulting solid was filtrated, dried, and recrystallized; otherwise, the aqueous solution was extracted with CH<sub>2</sub>Cl<sub>2</sub> (3 × 50 mL), the organic layers were dried (Na<sub>2</sub>SO<sub>4</sub>), and evaporated to dryness. The residue was purified by column chromatography using the appropriate eluent, to afford pure benzimidazoles **29**, **38**, **43**.

**4-Chloro-1H-benzimidazole (29).** Obtained from 3-chlorobenzene-1,2-diamine in quantitative yield; mp 167–169 °C (lit.<sup>42</sup> 170–171 °C) (EtOAc).

**5-(4-Methylpiperazin-1-yl)-1H-benzimidazole (38).** Obtained from **28** in 60% yield. Chromatography: CHCl<sub>3</sub>/MeOH, 95:5; mp 81–83 °C (lit.<sup>43</sup> 82–84 °C). Spectroscopic data are in agreement with those previously described.

**5-Piperazin-1-yl-1H-benzimidazole (43).** Obtained from **27** in 87% yield. Chromatography CHCl<sub>3</sub>/MeOH/NH<sub>3</sub> 6:4:0.1; mp 123–125 °C (lit.<sup>43</sup> 126–128 °C). Spectroscopic data are in agreement with those previously described.

**General Procedure for the Synthesis of Compounds 30 and 39.** To a suspension of K<sub>2</sub>CO<sub>3</sub> (2.86 g, 20.7 mmol) or NaH (444 mg, 11.1 mmol, 60% mineral oil) in anhydrous DMF (10 mL), **29** or **38** (6.9 mmol) was added portionwise, respectively, under an argon atmosphere. The mixture was stirred at room temperature for 1 h, then 2-(trimethylsilyl)ethoxymethyl chloride (SEMCl) (2.1 mL, 11.1 mmol) was added dropwise and the reaction was stirred for 2 h. The reaction was quenched with water and extracted with CH<sub>2</sub>Cl<sub>2</sub> (**30**) or EtOAc (**39**). The organic layers were dried (Na<sub>2</sub>SO<sub>4</sub>) and evaporated under vacuum, and the residue was purified by column chromatography, using the appropriate eluent, to provide **30** or **39**.

**4- and 7-Chloro-1-[[2-(trimethylsilyl)ethoxy]methyl]-1H-benzimidazoles (30).** Obtained from **29** in quantitative yield, as a nonseparable mixture of regioisomers in a 1:1 ratio. Chromatography: hexane/EtOAc, 7:3. IR (CHCl<sub>3</sub>) 1613, 1576, 1499, 1428. <sup>1</sup>H NMR (CDCl<sub>3</sub>) δ 0.03 (s, 9H), 0.93, 0.99 (br t, *J* = 4.5, 2H), 3.55, 3.62 (app t, *J* = 8.0, 2H), 5.59, 5.88 (s, 2H), 7.20–7.36 (m, 2H), 7.46, 7.72 (dd, *J* = 5.4, 1.0, 1H), 7.99, 8.03 (s, 1H). <sup>13</sup>C NMR (CDCl<sub>3</sub>) δ –1.4, –1.3, 17.8, 17.9, 66.3, 66.8, 74.6, 75.1, 109.2, 116.8, 119.4, 122.8, 123.4, 124.2, 125.0, 125.2, 130.1, 133.4, 143.4, 145.1, 146.3. MS (ESI) 283.0 (M + H).

**6-(4-Methylpiperazin-1-yl)-1-[[2-(trimethylsilyl)ethoxy]methyl]-1H-benzimidazole (39).** Obtained from **38** in 44% yield, after the separation from its 5-substituted regioisomer [Spectroscopic data of 5-(4-methylpiperazin-1-yl)-1-[[2-(trimethylsilyl)ethoxy]methyl]-1H-benzimidazole: IR (CHCl<sub>3</sub>) 1624, 1586, 1491, 1454. <sup>1</sup>H NMR (CDCl<sub>3</sub>) δ –0.05 (s, 9H), 0.90 (app t, *J* = 8.2, 2H), 2.39 (s, 3H), 2.65 (br t, *J* = 4.9, 4H), 3.24 (br t, *J* = 4.9, 4H), 3.50 (t, *J* = 8.2, 2H), 5.49 (s, 2H), 7.10 (dd, *J* = 8.8, 2.4, 1H), 7.34 (d, *J* = 2.1, 1H), 7.43 (d, *J* = 9.0, 1H), 7.90 (s, 1H). <sup>13</sup>C NMR (CDCl<sub>3</sub>) δ –1.6, 17.6, 46.0, 50.9, 55.2, 66.2, 74.2, 107.2, 110.2, 116.0, 128.3, 142.9, 144.9, 148.3. MS (EI) *m/z* (%) 346 (M, 100), 331 (21), 229 (21), 199 (9), 73 (46), 43 (40).] (38% yield) by column chromatography (CH<sub>2</sub>Cl<sub>2</sub>/EtOH, 9:1). IR (CHCl<sub>3</sub>) 1625, 1581, 1502, 1490, 1454. <sup>1</sup>H NMR (CDCl<sub>3</sub>) δ –0.03 (s, 9H), 0.91 (app t, *J* = 8.2, 2H), 2.39 (s, 3H), 2.64 (br t, *J* = 4.8, 4H), 3.26 (br t, *J* = 4.8, 4H), 3.51 (app t, *J* = 8.2, 2H), 5.49 (s, 2H), 7.00 (d, *J* = 2.1, 1H), 7.05 (dd, *J* = 9.0, 2.3, 1H), 7.69 (d, *J* = 8.8, 1H), 7.84 (s, 1H). <sup>13</sup>C NMR (CDCl<sub>3</sub>) δ –1.5, 17.6, 46.0, 50.5, 55.1, 66.2, 74.0, 96.9, 114.5, 120.4, 134.9, 137.9, 141.9, 149.5. MS (EI) *m/z* (%) 346 (M, 100), 331 (21), 229 (21), 199 (9), 73 (46), 43 (40).

**General Procedure for the Synthesis of Compounds 31 and 32.** To a solution of **30** (537 mg, 1.9 mmol) in *o*-xylene (17 mL) under an argon atmosphere, 1-BOC- or 1-methylpiperazine (2.7 mmol),

NaOt-Bu (250 mg, 2.7 mmol), tris(dibenzylideneacetone)dipalladium(0) (190 mg, 0.19 mmol), and tri-*t*-butylphosphine (150 mg, 0.8 mmol) were added. The mixture was heated at 110 °C for 24 h. Upon cooling to room temperature, the reaction was filtered over celite, the solvent was removed under reduced pressure, and the residue was purified by column chromatography using the appropriate eluent, to afford pure **31** or **32**.

**tert-Butyl 4-(1-[[2-(Trimethylsilyl)ethoxy]methyl]-1H-benzimidazol-4-yl)piperazine-1-carboxylate (31).** Obtained from **30** and 1-BOC-piperazine in 49% yield. Chromatography: hexane/EtOAc, 8:2. IR (CHCl<sub>3</sub>) 1697, 1603, 1543, 1477, 1450. <sup>1</sup>H NMR (CDCl<sub>3</sub>) δ –0.01 (s, 9H), 1.08 (app t, *J* = 8.6, 2H), 1.46 (s, 9H), 2.72 (br t, *J* = 4.8, 4H), 3.40–3.50 (m, 4H), 3.73 (app t, *J* = 8.3, 2H), 5.70 (s, 2H), 6.77 (dd, *J* = 8.0, 1.2, 1H), 7.26 (t, *J* = 8.0, 1H), 7.99 (dd, *J* = 8.4, 1.1, 1H), 8.04 (s, 1H). <sup>13</sup>C NMR (CDCl<sub>3</sub>, δ) –1.7, 18.1, 28.2, 51.8, 67.5, 75.3, 79.7, 114.7, 116.0, 125.0, 129.5, 138.0, 144.3, 149.9, 154.5.

**4-(4-Methylpiperazin-1-yl)-1-[[2-(trimethylsilyl)ethoxy]methyl]-1H-benzimidazole (32).** Obtained from **30** and 1-methylpiperazine in 43% yield. Chromatography: CH<sub>2</sub>Cl<sub>2</sub>/EtOH, 98:2. IR (CHCl<sub>3</sub>) 1499, 1453. <sup>1</sup>H NMR (CDCl<sub>3</sub>) δ –0.04 (s, 9H), 0.90 (app t, *J* = 8.4, 2H), 2.44 (s, 3H), 2.73 (br t, *J* = 4.8, 4H), 3.50 (app t, *J* = 8.1, 2H), 3.61 (m, 4H), 5.52 (s, 2H), 6.69 (d, *J* = 8.3, 1H), 7.12 (d, *J* = 8.3, 1H), 7.24 (t, *J* = 8.1, 1H), 7.90 (s, 1H). <sup>13</sup>C NMR (CDCl<sub>3</sub>, δ) –1.5, 17.8, 46.0, 52.8, 55.5, 65.9, 74.8, 115.3, 116.7, 122.8, 128.1, 139.9, 144.3, 145.4. MS (ESI) 347.0 (M + H).

**Synthesis of tert-Butyl 5- and 6-[4-tert-Butoxycarbonyl]piperazin-1-yl]-1H-benzimidazole-1-carboxylates (44).** To a solution of **43** (200 mg, 1 mmol) in anhydrous CH<sub>2</sub>Cl<sub>2</sub> (6 mL), di-*t*-butyl dicarbonate (648 mg, 3 mmol), triethylamine (0.4 mL, 3 mmol), and 4-(dimethylamino)pyridine (37 mg, 0.3 mmol) were added, and the mixture was stirred at room temperature overnight. The reaction solution was washed with 1 M NaOH and the organic layer was dried (Na<sub>2</sub>SO<sub>4</sub>) and evaporated at reduced pressure. The resulting crude was purified by column chromatography to give **44** in 69% yield, as a nonseparable mixture of regioisomers in a 1:1 ratio. IR (KBr) 1755, 1740, 1694, 1624, 1487, 1451. <sup>1</sup>H NMR (CDCl<sub>3</sub>) δ 1.50, 1.70 (s, 18H), 3.14–3.21, 3.62–3.66 (m, 8H), 7.05, 7.12 (dd, *J* = 8.9, 2.3, 1H), 7.31, 7.59 (br s, 1H), 7.66, 7.87 (d, *J* = 10.3, 1H), 8.30, 8.39 (s, 1H). <sup>13</sup>C NMR (CDCl<sub>3</sub>) δ 28.3, 28.6, 50.7, 51.1, 80.0, 85.4, 102.2, 108.2, 114.7, 115.9, 117.3, 120.9, 132.8, 133.0, 138.4, 140.2, 142.4, 147.6, 149.1, 149.7, 154.7. MS (EI) *m/z* (%) 402 (M, 18), 346 (44), 302 (24), 290 (100), 246 (50), 216 (23), 57 (45), 41 (37).

**General Procedure for the Synthesis of Compounds 33–37, 40–42, and 45.** To a solution of SEM-protected or BOC-protected benzimidazole **31**, **32**, **39**, or **44** (1.3 mmol) in anhydrous THF (5.2 mL), BuLi (1.8 mmol, 1.6 M in hexane) was added under an argon atmosphere at –78 °C. The mixture was stirred at this temperature for 1 h, then corresponding alkyl benzoate or naphthoate (1.4 mmol) was added slowly and the reaction mixture was allowed to reach room temperature and stirred overnight. The reaction was quenched with a saturated aqueous solution of NH<sub>4</sub>Cl, then extracted with CH<sub>2</sub>Cl<sub>2</sub>, and the organic layers were washed with water and brine, dried (Na<sub>2</sub>SO<sub>4</sub>), and evaporated to dryness. The residue was purified by column chromatography using the appropriate eluent, to afford pure **33–37**, **40–42**, **45**.

**tert-Butyl 4-(2-Benzoyl-1-[[2-(trimethylsilyl)ethoxy]methyl]-1H-benzimidazol-4-yl)piperazine-1-carboxylate (33).** Obtained from **31** and ethyl benzoate, in 21% yield. Chromatography: hexane/EtOAc, 8:2.

**[4-(4-Methylpiperazin-1-yl)-1-[[2-(trimethylsilyl)ethoxy]methyl]-1H-benzimidazol-2-yl](phenyl)methanone (34).** Obtained from **32** and ethyl benzoate, in 47% yield. Chromatography: CH<sub>2</sub>Cl<sub>2</sub>/EtOH, 95:5.

**tert-Butyl 4-[2-(1-Naphthoyl)-1-[[2-(trimethylsilyl)ethoxy]methyl]-1H-benzimidazol-4-yl]piperazine-1-carboxylate (35).** Obtained from **31** and ethyl 1-naphthoate in 27% yield. Chromatography:

hexane/EtOAc, 98:2.  $^1\text{H}$  NMR ( $\text{CDCl}_3$ )  $\delta$  -0.05 (s, 9H), 0.95 (app t,  $J = 8.3$ , 2H), 1.50 (s, 9H), 3.50 (m, 8H), 3.69 (app t,  $J = 8.3$ , 2H), 6.17 (s, 1H), 6.65 (d,  $J = 8.0$ , 1H), 7.21 (d,  $J = 8.4$ , 1H), 7.36 (t,  $J = 8.0$ , 1H), 7.51–7.58 (m, 3H), 7.93–7.96 (m, 1H), 8.10 (t,  $J = 8.9$ , 2H), 8.42–8.45 (m, 1H).  $^{13}\text{C}$  NMR ( $\text{CDCl}_3$ )  $\delta$  -1.3, 18.0, 28.5, 49.7, 66.5, 74.0, 79.8, 103.9, 108.3, 124.1, 125.7, 126.3, 127.6, 128.6, 131.5, 131.8, 132.9, 133.8, 134.3, 135.0, 138.1, 144.8, 144.9, 154.9, 188.7.

[4-(4-Methylpiperazin-1-yl)-1-[(2-(trimethylsilyl)ethoxy)methyl]-1H-benzimidazol-2-yl](1-naphthyl)methanone (36). Obtained from 32 and ethyl 1-naphthoate, in 55% yield. Chromatography:  $\text{CH}_2\text{Cl}_2/\text{EtOH}$ , 98:2.

[4-(4-Methylpiperazin-1-yl)-1-[(2-(trimethylsilyl)ethoxy)methyl]-1H-benzimidazol-2-yl](2-naphthyl)methanone (37). Obtained from 32 and methyl 2-naphthoate, in 59% yield. Chromatography:  $\text{CH}_2\text{Cl}_2/\text{EtOH}$ , 98:2.

[6-(4-Methylpiperazin-1-yl)-1-[(2-(trimethylsilyl)ethoxy)methyl]-1H-benzimidazol-2-yl](phenyl)methanone (40). Obtained from 39b and ethyl benzoate, in 63% yield. Chromatography:  $\text{CH}_2\text{Cl}_2/\text{EtOH}$ , 95:5.

[6-(4-Methylpiperazin-1-yl)-1-[(2-(trimethylsilyl)ethoxy)methyl]-1H-benzimidazol-2-yl](1-naphthyl)methanone (41). Obtained from 39b and ethyl 1-naphthoate, in 57% yield. Chromatography:  $\text{CH}_2\text{Cl}_2/\text{EtOH}$ , 95:5.

[6-(4-Methylpiperazin-1-yl)-1-[(2-(trimethylsilyl)ethoxy)methyl]-1H-benzimidazol-2-yl](2-naphthyl)methanone (42). Obtained from 39b and methyl 2-naphthoate, in 56% yield. Chromatography:  $\text{CH}_2\text{Cl}_2/\text{EtOH}$ , 97:3.  $^1\text{H}$  NMR ( $\text{CDCl}_3$ )  $\delta$  -0.11 (s, 9H), 1.02 (app t,  $J = 8.2$ , 2H), 2.52 (s, 3H), 2.80 (br t,  $J = 4.9$ , 4H), 3.48 (br t,  $J = 4.9$ , 4H), 3.76 (app t,  $J = 8.2$ , 2H), 6.16 (s, 2H), 7.13 (d,  $J = 2.0$ , 1H), 7.26 (dd,  $J = 9.1$ , 2.2, 1H), 7.60–7.75 (m, 2H), 7.92 (d,  $J = 9.0$ , 1H), 7.98–8.13 (m, 3H), 8.38 (dd,  $J = 8.6$ , 1.7, 1H), 9.03 (s, 1H).  $^{13}\text{C}$  NMR ( $\text{CDCl}_3$ )  $\delta$  -1.6, 17.7, 45.8, 49.5, 54.8, 66.2, 73.7, 96.3, 116.3, 122.2, 125.7, 126.4, 127.6, 127.9, 128.5, 129.9, 132.3, 133.7, 134.5, 135.6, 136.2, 137.3, 145.9, 150.7, 185.6.

*tert*-Butyl 4-[2-(2-Naphthyl)-1H-benzimidazol-5-yl]piperazine-1-carboxylate (45). Obtained from 44 and ethyl 2-naphthoate, in 33% yield. Chromatography: hexane/EtOAc, 9:1. IR ( $\text{CHCl}_3$ ) 3453, 3288, 1693, 1632, 1516, 1428.  $^1\text{H}$  NMR ( $\text{CDCl}_3$ )  $\delta$  1.52 (s, 9H), 3.24 (br t,  $J = 5.1$ , 4H), 3.64–3.67 (m, 4H), 6.95 (d,  $J = 2.1$ , 1H), 7.14 (dd,  $J = 9.1$ , 2.2, 1H), 7.56–7.68 (m, 2H), 7.87 (d,  $J = 9.3$ , 1H), 7.88 (d,  $J = 9.3$ , 1H), 7.98 (d,  $J = 8.7$ , 1H), 8.12 (d,  $J = 7.9$ , 1H), 8.53 (dd,  $J = 8.7$ , 1.7, 1H), 9.51 (s, 1H), 10.36 (br s, 1H).  $^{13}\text{C}$  NMR ( $\text{CDCl}_3$ )  $\delta$  28.3, 49.9, 50.4, 50.6, 79.9, 96.8, 116.6, 122.5, 125.6, 126.4, 127.6, 128.0, 128.6, 130.1, 132.4, 132.8, 134.0, 134.4, 135.7, 138.7, 147.3, 150.9, 154.6, 182.9. MS (EI)  $m/z$  (%) 456 (M, 36), 400 (77), 356 (33), 314 (100), 155 (29), 127 (36), 56 (32), 41 (25).

**General Procedure for the Synthesis of Benzimidazole Derivatives 1–8 (X = CO).** To a solution of 33–37, 40–42 (0.34 mmol) in freshly distilled  $\text{CH}_2\text{Cl}_2$  (3 mL),  $\text{BCl}_3$  (1.8 mmol, 1 M in  $\text{CH}_2\text{Cl}_2$ ) was added dropwise and under an argon atmosphere. The reaction was stirred at room temperature for 16 h, then quenched with saturated  $\text{NaHCO}_3$ . The reaction mixture was extracted with EtOAc, and the organic layers were dried ( $\text{Na}_2\text{SO}_4$ ) and evaporated at reduced pressure. The residue was purified by column chromatography using the appropriate eluent, to afford pure 1–8.

**Phenyl(4-piperazin-1-yl-1H-benzimidazol-2-yl)methanone (1).** Obtained from 33 in 58% yield. Chromatography:  $\text{CH}_2\text{Cl}_2/\text{MeOH}$ , 7:3; mp 123–125 °C.

[4-(4-Methylpiperazin-1-yl)-1H-benzimidazol-2-yl](phenyl)methanone (2). Obtained from 34 in 53% yield. Chromatography:  $\text{CH}_2\text{Cl}_2/\text{EtOH}$ , 98:2; mp 151–154 °C.

1-Naphthyl(4-piperazin-1-yl-1H-benzimidazol-2-yl)methanone (3). Obtained from 35 in 64% yield. Chromatography:  $\text{CH}_2\text{Cl}_2/\text{MeOH}$ , 7:3; mp 210–213 °C.

[4-(4-Methylpiperazin-1-yl)-1H-benzimidazol-2-yl](1-naphthyl)methanone (4). Obtained from 36 in 58% yield. Chromatography:  $\text{CH}_2\text{Cl}_2/\text{EtOH}$ , 9:1; mp 213–214 °C.

[4-(4-Methylpiperazin-1-yl)-1H-benzimidazol-2-yl](2-naphthyl)methanone (5). Obtained from 37 in 50% yield. Chromatography:  $\text{CH}_2\text{Cl}_2/\text{EtOH}$ , 98:2; mp 210–211 °C. IR (KBr) 3442, 3301, 1635, 1525, 1486, 1440.  $^1\text{H}$  NMR ( $\text{CDCl}_3$ )  $\delta$  2.47 (s, 3H), 2.83 (br t,  $J = 4.8$ , 4H), 3.81 (br t,  $J = 5.0$ , 4H), 6.67 (d,  $J = 7.7$ , 1H), 7.11 (d,  $J = 7.7$ , 1H), 7.32 (t,  $J = 8.0$ , 1H), 7.60–7.68 (m, 2H), 7.89–8.03 (m, 3H), 8.54 (dd,  $J = 8.7$ , 1.6, 1H), 9.78 (s, 1H), 10.50 (br s, 1H).  $^{13}\text{C}$  NMR ( $\text{CDCl}_3$ )  $\delta$  46.4, 49.9, 55.4, 104.4, 108.2, 126.1, 127.2, 127.9, 128.2, 128.4, 129.3, 130.5, 132.9, 133.1, 135.2, 135.5, 136.3, 136.6, 145.4, 145.9, 186.8. MS (ESI) 371.1 (M + H). Anal. ( $\text{C}_{23}\text{H}_{22}\text{N}_4\text{O}$ ) C, H, N.

[5-(4-Methylpiperazin-1-yl)-1H-benzimidazol-2-yl](phenyl)methanone (6). Obtained from 40 in 75% yield. Chromatography:  $\text{CHCl}_3/\text{MeOH}/\text{NH}_3$ , 9:1:0.1; mp 210–212 °C. IR (KBr) 3420, 3304, 1624, 1597, 1574, 1516, 1485, 1452.  $^1\text{H}$  NMR ( $\text{CDCl}_3$ )  $\delta$  2.40 (s, 3H), 2.65 (br t,  $J = 4.9$ , 4H), 3.31 (br t,  $J = 4.9$ , 4H), 6.91 (d,  $J = 2.1$ , 1H), 7.12 (dd,  $J = 9.1$ , 2.2, 1H), 7.53–7.58 (m, 2H), 7.62–7.67 (m, 1H), 7.81 (d,  $J = 9.1$ , 1H), 8.66 (dd,  $J = 7.0$ , 1.6, 2H), 10.60 (br s, 1H).  $^{13}\text{C}$  NMR ( $\text{CDCl}_3$ )  $\delta$  46.5, 50.1, 55.4, 96.8, 116.8, 122.9, 128.8, 131.5, 133.8, 135.2, 136.2, 138.9, 147.5, 150.5, 183.9. MS (ESI) 321.0 (M + H). Anal. ( $\text{C}_{19}\text{H}_{20}\text{N}_4\text{O}$ ) C, H, N.

[5-(4-Methylpiperazin-1-yl)-1H-benzimidazol-2-yl](1-naphthyl)methanone (7). Obtained from 41 in 77% yield. Chromatography:  $\text{CH}_2\text{Cl}_2/\text{EtOH}$ , 9:1; mp 142–144 °C.

[5-(4-Methylpiperazin-1-yl)-1H-benzimidazol-2-yl](2-naphthyl)methanone (8). Obtained from 42 in 65% yield. Chromatography:  $\text{CH}_2\text{Cl}_2/\text{EtOH}$ , 97:3; mp 231–233 °C. IR (KBr) 3444, 3299, 1633, 1616, 1570, 1517, 1493, 1446.  $^1\text{H}$  NMR ( $\text{CDCl}_3$ )  $\delta$  2.39 (s, 3H), 2.63 (br t,  $J = 4.8$ , 4H), 3.31 (br t,  $J = 4.8$ , 4H), 6.93 (d,  $J = 2.0$ , 1H), 7.13 (dd,  $J = 9.3$ , 2.0, 1H), 7.50–7.68 (m, 2H), 7.84 (d,  $J = 9.3$ , 1H), 7.90–7.98 (m, 2H), 8.10 (d,  $J = 7.8$ , 1H), 8.52 (dd,  $J = 8.6$ , 1.7, 1H), 9.48 (s, 1H), 10.23 (br s, 1H).  $^{13}\text{C}$  NMR ( $\text{CDCl}_3$ )  $\delta$  45.6, 48.8, 54.6, 96.0, 115.9, 121.6, 125.8, 126.9, 127.7, 127.9, 128.8, 129.9, 131.9, 132.9, 133.3, 135.0, 135.6, 137.6, 147.2, 150.3, 182.5. MS (ESI) 371.0 (M + H). Anal. ( $\text{C}_{23}\text{H}_{22}\text{N}_4\text{O}$ ) C, H, N.

**Synthesis of 2-Naphthyl-(5-piperazin-1-yl-1H-benzimidazol-2-yl)methanone (9).** To a solution of 45 (69 mg, 0.15 mmol) in anhydrous  $\text{CH}_2\text{Cl}_2$  (1 mL), trifluoroacetic acid (0.25 mL, 3 mmol) was added dropwise. The reaction mixture was stirred at room temperature for 5 h, then evaporated under reduced pressure. The resulting crude was resuspended in  $\text{CH}_2\text{Cl}_2$  and washed with 1 M NaOH. The organic layer was dried ( $\text{Na}_2\text{SO}_4$ ) and evaporated, and the obtained solid was purified by recrystallization from  $\text{Et}_2\text{O}$ , to afford pure 9 in quantitative yield; mp 155–157 °C. IR (KBr) 3442, 1626, 1600, 1516, 1461.  $^1\text{H}$  NMR ( $\text{CD}_3\text{OD}$ )  $\delta$  3.22–3.39 (m, 8H), 7.17 (br s, 1H), 7.23 (dd,  $J = 9.0$ , 2.2, 1H), 7.54–7.69 (m, 2H), 7.70 (d,  $J = 9.0$ , 1H), 7.95–8.09 (m, 3H), 8.29 (dd,  $J = 8.7$ , 1.7, 1H), 9.20 (s, 1H).  $^{13}\text{C}$  NMR ( $\text{CD}_3\text{OD}$ )  $\delta$  44.5, 49.2, 93.4, 111.7, 118.2, 125.6, 127.1, 127.9, 128.3, 129.0, 130.0, 132.0, 132.1, 132.8, 133.6, 133.8, 136.2, 148.2, 150.3, 183.9. MS (ESI) 357.0. Anal. ( $\text{C}_{22}\text{H}_{20}\text{N}_4\text{O}$ ) C, H, N.

**General Procedure for the Synthesis of Benzimidazole Derivatives 10–20 (X = CH<sub>2</sub>).** To a solution of previously synthesized 25–28 (1.5 mmol) and the appropriate aldehyde (2.3 mmol) in freshly distilled  $\text{CH}_2\text{Cl}_2$  (8 mL), ytterbium triflate (93 mg, 0.2 mmol) was added and the reaction was stirred at room temperature overnight. The mixture was filtered over celite, the solvent was evaporated under reduced pressure, and the residue was purified by column chromatography using the appropriate eluent, to afford pure 10–20.

2-Benzyl-4-piperazin-1-yl-1H-benzimidazole (10). Obtained from 25 and phenylacetaldehyde, in 45% yield. Chromatography:  $\text{CH}_2\text{Cl}_2/\text{EtOH}$ , 9:1; mp 126–128 °C.

2-Benzyl-4-(4-methylpiperazin-1-yl)-1H-benzimidazole (11). Obtained from 26 and phenylacetaldehyde, in 42% yield. Chromatography:  $\text{CH}_2\text{Cl}_2/\text{EtOH}$ , 8:2; mp 120–123 °C. IR (KBr) 3356, 1593, 1533, 1494, 1456.  $^1\text{H}$  NMR ( $\text{CDCl}_3$ )  $\delta$  2.44 (s, 3H), 2.79 (m, 4H), 3.62 (m, 4H), 4.30 (s, 2H), 6.66 (d,  $J = 8.0$ , 1H), 7.09 (m, 1H), 7.12 (t,  $J = 8.0$ , 1H), 7.30–7.38 (m, 5H).  $^{13}\text{C}$  NMR ( $\text{CDCl}_3$ )  $\delta$  36.3, 45.7, 49.6, 55.2, 105.6, 110.0, 123.6, 127.7, 129.4,

129.5, 135.1, 136.5, 137.0, 141.5, 151.3. MS (ESI) 307.0 (M + H). Anal. (C<sub>19</sub>H<sub>22</sub>N<sub>4</sub>) C, H, N.

**2-(1-Naphthylmethyl)-4-piperazin-1-yl-1H-benzimidazole (12).** Obtained from **25** and 1-naphthylacetaldehyde, in 45% yield. Chromatography: CH<sub>2</sub>Cl<sub>2</sub>/EtOH, 9:1; mp 163–165 °C. IR (KBr) 3454, 1617, 1597, 1531, 1455. <sup>1</sup>H NMR (CD<sub>3</sub>OD) δ 3.47–3.52 (m, 8H), 4.74 (s, 2H), 6.73–6.76 (m, 1H), 7.11–7.14 (m, 2H), 7.35 (d, *J* = 6.8, 1H), 7.42–7.50 (m, 3H), 7.83 (d, *J* = 8.2, 1H), 7.88–7.91 (m, 1H), 8.10–8.14 (m, 1H). <sup>13</sup>C NMR (CD<sub>3</sub>OD) δ 34.0, 45.3, 106.2, 108.7, 124.3, 124.7, 126.8, 127.1, 127.5, 128.3, 129.2, 129.9, 132.2, 134.2, 135.6, 136.2, 136.9, 142.2, 151.9. MS (ESI) 343.2 (M + H). Anal. (C<sub>22</sub>H<sub>22</sub>N<sub>4</sub>) C, H, N.

**4-(4-Methylpiperazin-1-yl)-2-(1-naphthylmethyl)-1H-benzimidazole (13).** Obtained from **26** and 1-naphthylacetaldehyde, in 48% yield. Chromatography: CH<sub>2</sub>Cl<sub>2</sub>/EtOH, 9:1; mp 95–96 °C.

**4-(4-Methylpiperazin-1-yl)-2-(2-naphthylmethyl)-1H-benzimidazole (14).** Obtained from **26** and 2-naphthylacetaldehyde, in 51% yield. Chromatography: CH<sub>2</sub>Cl<sub>2</sub>/EtOH, 8:2.

**2-Benzyl-5-piperazin-1-yl-1H-benzimidazole (15).** Obtained from **27** and phenylacetaldehyde, in 67% yield. Chromatography: CHCl<sub>3</sub>/MeOH/NH<sub>3</sub>, 9:1:0.1; mp 173–175 °C. IR (KBr) 3450, 1633, 1493, 1455. <sup>1</sup>H NMR (acetone-*d*<sub>6</sub>) δ 2.78–2.92 (m, 8H), 2.97 (br s, 1H), 4.05 (s, 2H), 6.76 (dd, *J* = 8.7, 2.3, 1H), 6.84 (d, *J* = 2.1, 1H), 7.07–7.25 (m, 6H), 7.90 (br s, 1H). <sup>13</sup>C NMR (acetone-*d*<sub>6</sub>) δ 35.7, 46.6, 52.6, 102.0, 114.3, 114.4, 126.9, 128.8, 129.2, 133.9, 136.1, 138.4, 149.3, 152.8. MS (ESI) 293.0 (M + H). Anal. (C<sub>18</sub>H<sub>20</sub>N<sub>4</sub>) C, H, N.

**2-Benzyl-5-(4-methylpiperazin-1-yl)-1H-benzimidazole (16).** Obtained from **28** and phenylacetaldehyde, in 53% yield. Chromatography: CH<sub>2</sub>Cl<sub>2</sub>/EtOH, 97:3; mp 108–109 °C.

**2-(1-Naphthylmethyl)-5-piperazin-1-yl-1H-benzimidazole (17).** Obtained from **27** and 1-naphthylacetaldehyde, in 44% yield. Chromatography: CH<sub>2</sub>Cl<sub>2</sub>/EtOH, 9:1; mp 112–114 °C.

**5-(4-Methylpiperazin-1-yl)-2-(1-naphthylmethyl)-1H-benzimidazole (18).** Obtained from **28** and 1-naphthylacetaldehyde, in 75% yield. Chromatography: CH<sub>2</sub>Cl<sub>2</sub>/EtOH, 9:1; mp 121–123 °C.

**2-(2-Naphthylmethyl)-5-piperazin-1-yl-1H-benzimidazole (19).** Obtained from **27** and 2-naphthylacetaldehyde, in 42% yield. Chromatography: CH<sub>2</sub>Cl<sub>2</sub>/EtOH 9:1; mp 157–159 °C. IR (KBr) 3443, 1632, 1490, 1456. <sup>1</sup>H NMR (CD<sub>3</sub>OD) δ 3.25–3.32 (m, 8H), 4.27 (s, 2H), 6.92 (dd, *J* = 8.8, 2.3, 1H), 7.02 (d, *J* = 2.0, 1H), 7.29–7.39 (m, 4H), 7.67–7.73 (m, 4H). <sup>13</sup>C NMR (CD<sub>3</sub>OD) δ 36.3, 45.3, 50.1, 103.9, 116.5, 116.7, 127.0, 127.5, 128.0, 128.5, 128.8, 129.7, 134.1, 135.3, 135.5, 135.8, 140.0, 148.6, 155.3. MS (ESI) 343.0 (M + H). Anal. (C<sub>22</sub>H<sub>22</sub>N<sub>4</sub>) C, H, N.

**5-(4-Methylpiperazin-1-yl)-2-(2-naphthylmethyl)-1H-benzimidazole (20).** Obtained from **28** and 2-naphthylacetaldehyde, in 59% yield. Chromatography: CH<sub>2</sub>Cl<sub>2</sub>/EtOH, 95:5; mp 149–152 °C.

**Pharmacology. Radioligand Binding Assays.** Membranes from HEK-293 cells expressing human 5-HT<sub>6</sub> or 5-HT<sub>7</sub> receptors, were purchased from Perkin-Elmer and conserved at –80 °C in packaging buffer for subsequent use. Specific radioligand [<sup>3</sup>H]LSD (79.2 Ci/mmol) was from NEN (Perkin-Elmer). Competitive inhibition assays were performed according to standard procedures, briefly detailed below.

**5-HT<sub>6</sub> Receptor.** Cell paste (6.0 mg/mL) was homogenized in 200 volumes of assay buffer (50 mM Tris-HCl, 10 mM MgCl<sub>2</sub>, 0.5 mM EDTA, pH 7.4 at 25 °C). Fractions of 20 μL of the membranes suspension were incubated at 37 °C for 60 min with 2.6 nM [<sup>3</sup>H]LSD, in the presence or absence of the competing drug, in a final volume of 200 μL of assay buffer. Nonspecific binding was determined by radioligand binding in the presence of a saturating concentration of 500 μM serotonin and represented less than 10% of total binding.

**5-HT<sub>7</sub> Receptor.** Cell paste (6.8 mg/mL) was homogenized in 200 volumes of assay buffer (50 mM Tris-HCl, 10 mM MgSO<sub>4</sub>, 0.5 mM EDTA, pH 7.4 at 25 °C). Fractions of 500 μL of the membranes suspension were incubated at 27 °C for 120 min with 3 nM [<sup>3</sup>H]LSD, in the presence or absence of the competing

drug, in a final volume of 540 μL of assay buffer. Nonspecific binding was determined by radioligand binding in the presence of a saturating concentration of 25 μM clozapine and represented less than 15% of total binding.

For all binding assays, competing drug, nonspecific, total, and radioligand bindings were defined in triplicate. Incubation was terminated by rapid vacuum filtration through Wallac Filtermat A filters, presoaked in poly(ethylenimine) (0.5% for the 5-HT<sub>6</sub>R and 0.3% for the 5-HT<sub>7</sub>R), using a FilterMate Unifilter 96-Harvester. The filters were then washed 5–9 times with 500 μL of ice-cold 50 mM Tris-HCl buffer (pH 7.4 at 25 °C) and heated at 80 °C. The radioactivity bound to the filters was measured by scintillation spectrometry, using a Microbeta TopCount instrument. The data were analyzed by an iterative curve-fitting procedure using GraphPad Prism, which provided IC<sub>50</sub>, *K<sub>i</sub>*, and *r*<sup>2</sup> values for test compounds, *K<sub>i</sub>* values being calculated from the Cheng–Prusoff equation.<sup>45</sup>

**Plasmid Construct.** HA-tagged-5-HT<sub>6</sub> receptor cDNAs in pRK5 were generated by fusing the sequence of the HA epitope (YPYDVPDYA) to a cleavable signal peptide (MVLILLISV-LLLKEDVRGSAQS) derived from the metabotropic glutamate receptor 5 (mGlu5R). This sequence was inserted into the pRK5 vector using Xba I and BsrG I restriction sites. Then, full-length mouse 5-HT<sub>6</sub>R cDNA was subcloned in frame using BsrG I and Hind III. HA-5-HT<sub>6</sub>-C3.36A, HA-5-HT<sub>6</sub>-S5.43A, HA-5-HT<sub>6</sub>-W6.48A, HA-5-HT<sub>6</sub>-F6.52A, HA-5-HT<sub>6</sub>-N6.55A receptor mutants were generated from HA-5-HT<sub>6</sub>R, cloned in pRK5, with the Quick Change Site-Directed Mutagenesis kit (Stratagene, Amsterdam, Netherlands).

**Cell Surface ELISA.** COS-7 cells were transfected with HA-tagged-5-HT<sub>6</sub>R, WT or mutants cDNAs. Cells were grown on 96-well plates in DMEM medium with 10% dFCS and fixed as described previously.<sup>63</sup> Cells were then incubated with anti-HA antibody at 0.6 μg/mL for 60 min in the same buffer and incubated with antirabbit/HRP conjugate (Amersham Pharmacia Biotech) at 1 μg/mL for 60 min. Chromogenic substrate was added (Supersignal ELISA femto-maximum sensitivity, Pierce, Perbio-Brebières, France). Chemiluminescence was detected and quantified by a Wallac Victor2 luminescence counter.

**Determination of cAMP Production in Transfected Cells.** COS-7 cells were transfected with the appropriate cDNA and seeded into 24-well plates (100000 cells/well). Twenty-four hours post-transfection, a 10 min-stimulation with the appropriate concentrations of each tested compound in absence or presence of 100 μM 5-HT was performed as previously described.<sup>61</sup> Quantification of cAMP production was performed by homogeneous time-resolved fluorescence (HTRF) using the cAMP Dynamic kit (Cisbio International, Bagnols-sur-Cèze, France), according to the manufacturer's instructions.

**Data Analysis.** The dose–response curves were fitted using GraphPad Prism and the following equation for monophasic dose–response curves:  $y = (y_{\max} - y_{\min}) / (1 + [(x/IC_{50})^{n_H}] + y_{\min})$ , where IC<sub>50</sub> is the concentration of the antagonist necessary to reduce 50% of the maximal effect induced by 5-HT and *n<sub>H</sub>* is the Hill coefficient. All data represented correspond to the mean ± SEM of three independent experiments performed in triplicate.

**Computational Methods. Models of the Ligand–Receptor Complexes.** Modeler v9.5<sup>64</sup> was used to build a homology model of the human 5-HT<sub>6</sub>R using the crystal structure of the β<sub>2</sub>-adrenergic receptor (PDB code 2RH1)<sup>47,65</sup> as template. Internal water molecules 506, 519, 528, 529, 532, 534, 537, 543, 546, and 548 that mediate a number of interhelical interactions,<sup>48</sup> and seem conserved in the rhodopsin-like family of GPCRs,<sup>66</sup> were also included in the model. The Duan et al. (2003) force field<sup>67</sup> was used for receptors and the general Amber force field (GAFF)<sup>68</sup> and HF/6-31G\*-derived RESP atomic charges were used for the ligands. Molecular dynamics simulations of the ligand–receptor complexes were performed with the Sander module of AMBER 9<sup>69</sup> using the protocol previously described.<sup>70</sup>

**Acknowledgment.** This work has been supported by grants from the Spanish Ministerio de Educación (MEC, SAF-2007/67008), Comunidad Autónoma de Madrid (CAM, S-SAL-249-2006), and Instituto de Salud Carlos III (RD07/0067/0008). We thank the Fundación Ramón Areces and MEC for predoctoral grants to T.F., J.S., and R.A.M.

**Supporting Information Available:** Spectral characterization data of compounds 1–4, 7, 10, 13, 14, 16–18, 20, 25, 27, 29, 33, 34, 36, 37, 40, and 41; combustion analysis data. This material is available free of charge via the Internet at <http://pubs.acs.org>.

## References

- Vialli, M.; Erspamer, V. Z. Cellule enterocromaffini e cellule basigranulose acidofile nei vertebrati. *Zellforsch. Mikrosk. Anat.* **1933**, *19*, 743.
- Rapport, M. M.; Green, A. A.; Page, I. H. Serum vasoconstrictor, serotonin; isolation and characterization. *J. Biol. Chem.* **1948**, *176*, 1243–1251.
- Adayev, T.; Ranasinghe, B.; Banerjee, P. Transmembrane signaling in the brain by serotonin, a key regulator of physiology and emotion. *Biosci. Rep.* **2005**, *25*, 363–385.
- Slassi, A.; Isaac, M.; O'Brien, A. Recent progress in 5-HT<sub>6</sub> receptor antagonists for the treatment of CNS diseases. *Expert Opin. Ther. Pat.* **2002**, *12*, 513–527.
- Uphouse, L. Multiple serotonin receptors: too many, not enough, or just the right number? *Neurosci. Biobehav. Rev.* **1997**, *21*, 679–698.
- Hoyer, D.; Martin, G. 5-HT receptor classification and nomenclature: towards a harmonization with the human genome. *Neuropharmacology* **1997**, *36*, 419–428.
- Bartfai, T.; Benovic, J. L.; Bockaert, J.; Bond, R. A.; Bouvier, M.; Christopoulos, A.; Civelli, O.; Devi, L. A.; George, S. R.; Inui, A.; Kobilka, B.; Leurs, R.; Neubig, R.; Pin, J. P.; Quiroion, R.; Roques, B. P.; Sakmar, T. P.; Seifert, R.; Stenkamp, R. E.; Strange, P. G. The state of GPCR research in 2004. *Nature Rev. Drug Discovery* **2004**, *3*, 577–626.
- Filizola, M.; Weinstein, H. The structure and dynamics of GPCR oligomers: a new focus in models of cell-signaling mechanisms and drug design. *Curr. Opin. Drug Discovery Dev.* **2005**, *8*, 577–584.
- Landry, Y.; Niederhoffer, N.; Sick, E.; Gies, J. P. Heptahelical and other G-protein-coupled receptors (GPCRs) signaling. *Curr. Med. Chem.* **2006**, *13*, 51–63.
- Rosenbaum, D. M.; Rasmussen, S. G.; Kobilka, B. K. The structure and function of G-protein-coupled receptors. *Nature* **2009**, *459*, 356–363.
- FDA Approved Drug Products: <http://www.accessdata.fda.gov/Scripts/cder/DrugsatFDA/> (accessed January 2010).
- Kohen, R.; Metcalf, M. A.; Druck, T.; Huebner, K.; Sibley, D. R.; Hamblin, M. W. Cloning and chromosomal localization of a human 5-HT<sub>6</sub> serotonin receptor. *Soc. Neurosci. Abstr.* **1994**, *20*, 476.8.
- Kohen, R.; Metcalf, M. A.; Khan, N.; Druck, T.; Huebner, K.; Lachowicz, J. E.; Meltzer, H. Y.; Sibley, D. R.; Roth, B. L.; Hamblin, M. W. Cloning, characterization, and chromosomal localization of a human 5-HT<sub>6</sub> serotonin receptor. *J. Neurochem.* **1996**, *66*, 47–56.
- Kohen, R.; Fashingbauer, L. A.; Heidmann, D. E.; Guthrie, C. R.; Hamblin, M. W. Cloning of the mouse 5-HT<sub>6</sub> serotonin receptor and mutagenesis studies of the third cytoplasmic loop. *Brain Res. Mol. Brain Res.* **2001**, *90*, 110–117.
- Plassat, J. L.; Amlaiky, N.; Hen, R. Molecular cloning of a mammalian serotonin receptor that activates adenylate cyclase. *Mol. Pharmacol.* **1993**, *44*, 229–236.
- Sebben, M.; Ansanay, H.; Bockaert, J.; Dumuis, A. 5-HT<sub>6</sub> receptors positively coupled to adenylyl cyclase in striatal neurones in culture. *Neuroreport* **1994**, *5*, 2553–2557.
- Max, S. I.; Monsma, F. J., Jr.; Sibley, D. R. Agonist-induced desensitization of 5-HT<sub>6</sub> serotonin receptor-coupled adenylyl cyclase in stably transfected HEK-293 cells. *J. Serotonin Res.* **1995**, *2*, 101–116.
- Monsma, F. J., Jr.; Shen, Y.; Ward, R. P.; Hamblin, M. W.; Sibley, D. R. Cloning and expression of a novel serotonin receptor with high affinity for tricyclic psychotropic drugs. *Mol. Pharmacol.* **1993**, *43*, 320–327.
- Davies, S. L.; Silvestre, J. S.; Guitart, X. Drug discovery targets: 5-HT<sub>6</sub> receptor. *Drugs Future* **2005**, *30*, 479–495.
- Bourson, A.; Borroni, E.; Austin, R. H.; Monsma, F. J., Jr.; Sleight, A. J. Determination of the role of the 5-HT<sub>6</sub> receptor in the rat brain: a study using antisense oligonucleotides. *J. Pharmacol. Exp. Ther.* **1995**, *274*, 173–180.
- Sleight, A. J.; Boess, F. G.; Monsma, F. J.; Bourson, A. 5-HT<sub>6</sub> and 5-HT<sub>7</sub> receptors: new targets for neuropsychiatry. *Eur. Neuropsychopharmacol.* **1996**, *6*, S4.
- Holenz, J.; Pauwels, P. J.; Diaz, J. L.; Merce, R.; Codony, X.; Buschmann, H. Medicinal chemistry strategies to 5-HT(6) receptor ligands as potential cognitive enhancers and antiobesity agents. *Drug Discovery Today* **2006**, *11*, 283–299.
- Mitchell, E. S.; Neumaier, J. F. 5-HT<sub>6</sub> receptors: a novel target for cognitive enhancement. *Pharmacol. Ther.* **2005**, *108*, 320–333.
- Svartengren, J.; Axelsson-Lendin, P.; Edling, N.; Fhoelnhag, K.; Isacson, R.; Hillegaard, V.; Groenberg, A. The selective serotonin 5-HT<sub>6</sub> receptor antagonist BVT5182 decreases food intake and body weight in both rats and mice. *34th Annu. Meet. Soc. Neurosci.* **2004**, Abs 75.8.
- Gannon, K. S.; Heal, D. J.; Cheetham, S. C.; Jackson, H. C.; Seeley, R. J.; Melendez, R. PRX-07034, a potent and selective 5-HT<sub>6</sub> receptor antagonist reduces food intake and body weight in rats. *Proceedings of the Serotonin Club Sixth IUPHAR Satellite Meeting on Serotonin, Hokkaido* **2006**, P2–P17.
- Heal, D. J.; Smith, S. L.; Fisas, A.; Codony, X.; Buschmann, H. Selective 5-HT<sub>6</sub> receptor ligands: progress in the development of a novel pharmacological approach to the treatment of obesity and related metabolic disorders. *Pharmacol. Ther.* **2008**, *117*, 207–231.
- Glennon, R. A. Higher-end serotonin receptors: 5-HT(5), 5-HT(6), and 5-HT(7). *J. Med. Chem.* **2003**, *46*, 2795–2812.
- Ruat, M.; Traiffort, E.; Arrang, J. M.; Tardivel-Lacombe, J.; Diaz, J.; Leurs, R.; Schwartz, J. C. A novel rat serotonin (5-HT<sub>6</sub>) receptor: molecular cloning, localization and stimulation of cAMP accumulation. *Biochem. Biophys. Res. Commun.* **1993**, *193*, 268–276.
- Gerard, C.; Martres, M. P.; Lefevre, K.; Miquel, M. C.; Verge, D.; Lanfumey, L.; Doucet, E.; Hamon, M.; el Mestikawy, S. Immunolocalization of serotonin 5-HT<sub>6</sub> receptor-like material in the rat central nervous system. *Brain Res.* **1997**, *746*, 207–219.
- Sleight, A. J.; Boess, F. G.; Bos, M.; Levet-Trafit, B.; Bourson, A. The 5-hydroxytryptamine(6) receptor: localisation and function. *Exp. Opin. Ther. Patents* **1998**, *8*, 1217–1224.
- Hirst, W. D.; Abrahamsen, B.; Blaney, F. E.; Calver, A. R.; Aloj, L.; Price, G. W.; Medhurst, A. D. Differences in the central nervous system distribution and pharmacology of the mouse 5-hydroxytryptamine-6 receptor compared with rat and human receptors investigated by radioligand binding, site-directed mutagenesis, and molecular modeling. *Mol. Pharmacol.* **2003**, *64*, 1295–1308.
- Sleight, A. J.; Boess, F. G.; Bos, M.; Levet-Trafit, B.; Riemer, C.; Bourson, A. Characterization of Ro 04-6790 and Ro 63-0563: potent and selective antagonists at human and rat 5-HT<sub>6</sub> receptors. *Br. J. Pharmacol.* **1998**, *124*, 556–562.
- Bromidge, S. M.; Brown, A. M.; Clarke, S. E.; Dodgson, K.; Gager, T.; Grassam, H. L.; Jeffrey, P. M.; Joiner, G. F.; King, F. D.; Middlemiss, D. N.; Moss, S. F.; Newman, H.; Riley, G.; Routledge, C.; Wyman, P. 5-Chloro-N-(4-methoxy-3-piperazinyl-phenyl)-3-methyl-2-benzothiophenesulfonamide (SB-271046): a potent, selective, and orally bioavailable 5-HT<sub>6</sub> receptor antagonist. *J. Med. Chem.* **1999**, *42*, 202–205.
- Glennon, R. A.; Bondarev, M.; Roth, B. L. 5-HT<sub>6</sub> serotonin receptor binding of indolealkylamines: A preliminary structure–affinity investigation. *Med. Chem. Res.* **1999**, *9*, 108–117.
- Glennon, R. A.; Lee, M.; Rangisetty, J. B.; Dukat, M.; Roth, B. L.; Savage, J. E.; McBride, A.; Rauser, L.; Hufesein, S.; Lee, D. K. H. 2-Substituted tryptamines: agents with selectivity for 5-HT(6) serotonin receptors. *J. Med. Chem.* **2000**, *43*, 1011–1018.
- Tsai, Y.; Dukat, M.; Slassi, A.; MacLean, N.; Demchyshyn, L.; Savage, J. E.; Roth, B. L.; Hufesein, S.; Lee, M.; Glennon, R. A. N<sub>1</sub>-(Benzenesulfonyl)tryptamines as novel 5-HT<sub>6</sub> antagonists. *Bioorg. Med. Chem. Lett.* **2000**, *10*, 2295–2299.
- Lee, M.; Rangisetty, J. B.; Dukat, M.; Slassi, A.; Maclean, N.; Lee, D. K. H.; Glennon, R. A. 5-HT<sub>6</sub> serotonin receptor binding affinities of N<sub>1</sub>-benzenesulfonyl and related tryptamines. *Med. Chem. Res.* **2000**, *10*, 230–242.
- Russell, M. G.; Baker, R. J.; Barden, L.; Beer, M. S.; Bristow, L.; Broughton, H. B.; Knowles, M.; McAllister, G.; Patel, S.; Castro, J. L. N-Arylsulfonylindole derivatives as serotonin 5-HT(6) receptor ligands. *J. Med. Chem.* **2001**, *44*, 3881–3895.
- Catalyst, version 4.9*; Molecular Simulations Inc.: San Diego, CA, 2003.
- Lopez-Rodriguez, M. L.; Benhamu, B.; de la Fuente, T.; Sanz, A.; Pardo, L.; Campillo, M. A three-dimensional pharmacophore

- model for 5-hydroxytryptamine<sub>6</sub> (5-HT<sub>6</sub>) receptor antagonists. *J. Med. Chem.* **2005**, *48*, 4216–4219.
- (41) Montanari, F.; Manzini, A. Ricerche sui benzimidazoli. *Boll. Fac. Chim. Ind. Bologna* **1953**, *11*, 42–50.
- (42) Dandegaonker, S. H.; Revankar, G. R. 4(7)-Halobenzimidazoles. *J. Karnatak Univ.* **1961**, *6*, 25–32.
- (43) Lopez-Rodriguez, M. L.; Benhamu, B.; Ayala, D.; Rominguera, J. L.; Murcia, M.; Ramos, J. A.; Viso, A. Pd(0) Amination of benzimidazoles as an efficient method towards new (benzimidazolyl)piperazines with high affinity for the 5-HT<sub>1A</sub> receptor. *Tetrahedron* **2000**, *56*, 3245–3253.
- (44) Sanchez-Alonso, R. M.; Ravina, E.; Santana, L.; Garcia-Mera, G.; Sanmartin, M.; Baltar, P. Piperazine derivatives of benzimidazole as potential anthelmintics. Part I: Synthesis and activity of methyl-5-(4-substituted piperazin-1-yl)benzimidazole-2-carbamates. *Pharmazie* **1989**, *44*, 606–607.
- (45) Cheng, Y. C.; Prusoff, W. H. Relationship between the inhibition constant ( $K_i$ ) and the concentration of inhibitor which causes 50% inhibition ( $I_{50}$ ) of an enzymatic reaction. *Biochem. Pharmacol.* **1973**, *22*, 3099–3108.
- (46) Warne, T.; Serrano-Vega, M. J.; Baker, J. G.; Moukhametzianov, R.; Edwards, P. C.; Henderson, R.; Leslie, A. G.; Tate, C. G.; Schertler, G. F. Structure of a  $\beta_1$ -adrenergic G-protein-coupled receptor. *Nature* **2008**, *454*, 486–491.
- (47) Cherezov, V.; Rosenbaum, D. M.; Hanson, M. A.; Rasmussen, S. G.; Thian, F. S.; Kobilka, T. S.; Choi, H. J.; Kuhn, P.; Weis, W. I.; Kobilka, B. K.; Stevens, R. C. High-resolution crystal structure of an engineered human  $\beta_2$ -adrenergic G protein-coupled receptor. *Science* **2007**, *318*, 1258–1265.
- (48) Rosenbaum, D. M.; Cherezov, V.; Hanson, M. A.; Rasmussen, S. G.; Thian, F. S.; Kobilka, T. S.; Choi, H. J.; Yao, X. J.; Weis, W. I.; Stevens, R. C.; Kobilka, B. K. GPCR engineering yields high-resolution structural insights into  $\beta_2$ -adrenergic receptor function. *Science* **2007**, *318*, 1266–1273.
- (49) Shi, L.; Javitch, J. A. The binding site of aminergic G protein-coupled receptors: the transmembrane segments and second extracellular loop. *Annu. Rev. Pharmacol. Toxicol.* **2002**, *42*, 437–467.
- (50) Pullagurla, M. R.; Westkaemper, R. B.; Glennon, R. A. Possible differences in modes of agonist and antagonist binding at human 5-HT<sub>6</sub> receptors. *Bioorg. Med. Chem. Lett.* **2004**, *14*, 4569–4573.
- (51) Dukat, M.; Mosier, P. D.; Kolanos, R.; Roth, B. L.; Glennon, R. A. Binding of serotonin and N<sub>1</sub>-benzenesulfonyltryptamine-related analogs at human 5-HT<sub>6</sub> serotonin receptors: Receptor modeling studies. *J. Med. Chem.* **2008**, *51*, 603–611.
- (52) Smit, M. J.; Vischer, H. F.; Bakker, R. A.; Jongejan, A.; Timmerman, H.; Pardo, L.; Leurs, R. Pharmacogenomic and structural analysis of constitutive G protein-coupled receptor activity. *Annu. Rev. Pharmacol. Toxicol.* **2007**, *47*, 53–87.
- (53) Nygaard, R.; Frimurer, T. M.; Holst, B.; Rosenkilde, M. M.; Schwartz, T. W. Ligand binding and micro-switches in 7TM receptor structures. *Trends Pharmacol. Sci.* **2009**, *30*, 249–259.
- (54) Schwartz, T. W.; Frimurer, T. M.; Holst, B.; Rosenkilde, M. M.; Elling, C. E. Molecular mechanism of 7TM receptor activation—a global toggle switch model. *Annu. Rev. Pharmacol. Toxicol.* **2006**, *46*, 481–519.
- (55) Ozawa, T.; Tsuji, E.; Ozawa, M.; Handa, C.; Mukaiyama, H.; Nishimura, T.; Kobayashi, S.; Okazaki, K. The importance of CH/ $\pi$  hydrogen bonds in rational drug design: An ab initio fragment molecular orbital study to leukocyte-specific protein tyrosine (LCK) kinase. *Bioorg. Med. Chem.* **2008**, *16*, 10311–10318.
- (56) Swaminath, G.; Xiang, Y.; Lee, T. W.; Steenhuis, J.; Parnot, C.; Kobilka, B. K. Sequential binding of agonists to the  $\beta_2$  adrenoceptor. Kinetic evidence for intermediate conformational states. *J. Biol. Chem.* **2004**, *279*, 686–691.
- (57) Crocker, E.; Eilers, M.; Ahuja, S.; Hornak, V.; Hirshfeld, A.; Sheves, M.; Smith, S. O. Location of Trp265 in metarhodopsin II: implications for the activation mechanism of the visual receptor rhodopsin. *J. Mol. Biol.* **2006**, *357*, 163–172.
- (58) Ruprecht, J. J.; Mielke, T.; Vogel, R.; Villa, C.; Schertler, G. F. Electron crystallography reveals the structure of metarhodopsin I. *EMBO J.* **2004**, *23*, 3609–3620.
- (59) Lopez-Rodriguez, M. L.; Morcillo, M. J.; Fernandez, E.; Benhamu, B.; Tejada, I.; Ayala, D.; Viso, A.; Campillo, M.; Pardo, L.; Delgado, M.; Manzanares, J.; Fuentes, J. A. Synthesis and structure–activity relationships of a new model of arylpiperazines. 8. Computational simulation of ligand–receptor interaction of 5-HT<sub>1A</sub>R agonists with selectivity over  $\alpha_1$ -adrenoceptors. *J. Med. Chem.* **2005**, *48*, 2548–2558.
- (60) Pellissier, L. P.; Sallander, J.; Campillo, M.; Gaven, F.; Queffeuol, E.; Pillot, M.; Dumuis, A.; Claeysen, S.; Bockaert, J.; Pardo, L. Conformational toggle switches implicated in basal constitutive and agonist-induced activated states of 5-HT<sub>4</sub> receptors. *Mol. Pharmacol.* **2009**, *75*, 982–990.
- (61) Abuzari, S.; Sharma, S. Synthesis of 2-carbalkoxyamino-5(6)-(1-substituted piperazin-4-yl)piperazin-4-ylcarbonyl)benzimidazoles and related compounds as potential anthelmintics. *Pharmazie* **1984**, *39*, 747–749.
- (62) Kelly, D. P.; Bateman, S. A.; Martin, R. F.; Reum, M. E.; Rose, M.; Whittaker, A. R. D. DNA Binding compounds. V Synthesis and characterization of boron-containing bibenzimidazoles related to the DNA minor groove binder, Hoechst 332585. *Aust. J. Chem.* **1994**, *47*, 247–262.
- (63) Barthet, G.; Gaven, F.; Framery, B.; Shinjo, K.; Nakamura, T.; Claeysen, S.; Bockaert, J.; Dumuis, A. Uncoupling and endocytosis of 5-hydroxytryptamine 4 receptors. Distinct molecular events with different GRK2 requirements. *J. Biol. Chem.* **2005**, *280*, 27924–27934.
- (64) Marti-Renom, M. A.; Stuart, A. C.; Fiser, A.; Sanchez, R.; Melo, F.; Sali, A. Comparative protein structure modeling of genes and genomes. *Annu. Rev. Biophys. Biomol. Struct.* **2000**, *29*, 291–325.
- (65) Rasmussen, S. G.; Choi, H. J.; Rosenbaum, D. M.; Kobilka, T. S.; Thian, F. S.; Edwards, P. C.; Burghammer, M.; Ratnala, V. R.; Sanishvili, R.; Fischetti, R. F.; Schertler, G. F.; Weis, W. I.; Kobilka, B. K. Crystal structure of the human  $\beta_2$  adrenergic G-protein-coupled receptor. *Nature* **2007**, *450*, 383–387.
- (66) Pardo, L.; Deupi, X.; Dolker, N.; Lopez-Rodriguez, M. L.; Campillo, M. The role of internal water molecules in the structure and function of the rhodopsin family of G protein-coupled receptors. *ChemBioChem* **2007**, *8*, 19–24.
- (67) Duan, Y.; Wu, C.; Chowdhury, S.; Lee, M. C.; Xiong, G.; Zhang, W.; Yang, R.; Cieplak, P.; Luo, R.; Lee, T.; Caldwell, J.; Wang, J.; Kollman, P. A point-charge force field for molecular mechanics simulations of proteins based on condensed-phase quantum mechanical calculations. *J. Comput. Chem.* **2003**, *24*, 1999–2012.
- (68) Wang, J.; Wolf, R. M.; Caldwell, J. W.; Kollman, P. A.; Case, D. A. Development and testing of a general Amber force field. *J. Comput. Chem.* **2004**, *25*, 1157–1174.
- (69) Case, D. A.; Darden, T. A.; Cheatham, T. E. I.; Simmerling, C. L.; Wang, J.; Duke, R. E.; Luo, R.; Merz, K. M.; Pearlman, D. A.; Crowley, M.; Walker, R. C.; Zhang, W.; Wang, B.; Hayik, S.; Roitberg, A.; Seabra, G.; Wong, K. F.; Paesani, F.; Wu, X.; Brozell, S.; Tsui, V.; Gohlke, H.; Yang, L.; Tan, C.; Mongan, J.; Hornak, V.; Cui, G.; Beroza, P.; Mathews, D. H.; Schafmeister, C.; Ross, W. S.; Kollman, P. A. *AMBER 9*; University of California: San Francisco, 2006.
- (70) Jongejan, A.; Bruysters, M.; Ballesteros, J. A.; Haaksmma, E.; Bakker, R. A.; Pardo, L.; Leurs, R. Linking agonist binding to histamine H<sub>1</sub> receptor activation. *Nat. Chem. Biol.* **2005**, *1*, 98–103.